

Origin, HP/LT metamorphism and cooling of ophiolitic mélanges in southern Evia (NW Cyclades), Greece

Y. KATZIR,^{1*} D. AVIGAD,¹ A. MATTHEWS,¹ Z. GARFUNKEL¹ AND B. W. EVANS²

¹Institute of Earth Sciences, The Hebrew University of Jerusalem, Jerusalem 91904, Israel (yaron@geology.wisc.edu)

²Department of Geological Sciences, University of Washington, Seattle, WA 98195-1310, USA

ABSTRACT Basic and ultrabasic blocks within ophiolitic mélanges of the Cycladic Blueschist Unit in southern Evia provide a detailed insight into its ocean floor igneous and hydrothermal evolution, as well as the regional poly-metamorphism occurring during Alpine orogenesis. The upper structural levels (Mt. Ochi exposures) are dominated by metamorphosed wehrlites, gabbros and highly light rare earth element (LREE)-enriched pillow basalts, whereas the underlying Tsaki mélange consists of basic protoliths with much less fractionated REE patterns as well as mantle harzburgites. Most of the metabasites show Nb anomalies, indicative of derivation from a subduction-affected mantle. The igneous bodies were juxtaposed and incorporated into the enclosing sedimentary sequences prior to high-pressure/low-temperature (HP/LT) metamorphism (M1). Glaucophane, epidote, sodic clinopyroxene and high-Si phengite constitute the Eocene M1 assemblage, which is estimated to have formed at >11 kbar and 400–450 °C. High $\delta^{18}\text{O}$ values of M1 minerals in Ochi metagabbros indicate that the formation of the high-pressure assemblage was controlled by infiltration of fluids from the dehydrating host sediments. Cooling during decompression is indicated by an overprinting (M2, Early Miocene) pumpellyite–actinolite facies assemblage in metabasic rocks, calculated to have developed at $P < 8$ kbar and $T < 350$ °C. Possible mechanisms for such cooling include: exhumation from shallower burial levels relative to the eclogites of the NW Cyclades, accretion of colder rocks from below and extensional unroofing by low-angle normal faults and detachments. The occurrence of sodic augite in the M2 assemblage of Tsaki metagabbros indicates that rocks at the base of the Blueschist Unit cooled faster or longer than their higher level Ochi counterparts. This suggests that differential cooling of the blueschists was enhanced by the underthrusting of colder rock units.

Key words: Cyclades; HP/LT metamorphism; mélange; ophiolite.

INTRODUCTION

Considerable knowledge of the deep tectono-thermal evolution of orogenic terranes comes from the study of high-pressure/low-temperature (HP/LT) metamorphic rocks. Blueschists and eclogites may sample a wide range of geotectonic processes, including the creation and hydrothermal alteration of the ocean floor, the juxtaposition of rocks in an accretionary wedge, subduction and metamorphism and, finally, exhumation. Lower grade blueschist terranes, in particular, may preserve a geological record of the mineral assemblages, rocks and structures that formed prior to high-pressure metamorphism. The Attic-Cycladic Massif (Fig. 1) is a well-studied orogenic terrane that records a cycle of Alpine collisional thickening, followed by extensional collapse and overprinting by back-arc extension, that has resulted in widespread exposures of HP/LT metamorphic rocks (Ridley, 1984; Avigad & Garfunkel, 1991; Gautier & Brun, 1994). Among the HP/LT exposures are those occurring on

the southern parts of the island of Evia, where sporadically distributed, lower grade, lawsonite-bearing blueschist facies rocks are found (Bavay & Romain-Bavay, 1980; Blake *et al.*, 1981; Bonneau & Kienast, 1982; Reinecke, 1986). These occurrences contrast with HP/LT rocks found in the more interior parts of the Massif on the islands of Sifnos, Tinos and Syros, where eclogite facies metamorphism frequently obliterated the petrological record of earlier processes. A significant exception occurs on Syros where pre-HP/LT mineral relics are preserved in the metagabbros of an ophiolitic mélange (Dixon & Ridley, 1987). Pre-HP/LT relics are also preserved in ophiolitic mélanges occurring within the blueschist sequence of southern Evia and, together with the low grade of metamorphism, allow an exploration of the origin and evolution of the Attic-Cycladic Massif.

In this work, we use the unique characteristics of southern Evian HP/LT rocks to address three major aspects of orogenic evolution.

1 The metamorphosed ophiolitic mélanges on Evia are composed of blocks of igneous oceanic origin enclosed within metasedimentary host rocks. The excellent preservation of the igneous structures (e.g. pillows, dykes, cumulates) in Evian blueschists,

*Present address: Department of Geology and Geophysics, University of Wisconsin, 1215 W. Dayton St, Madison, WI 53706, USA

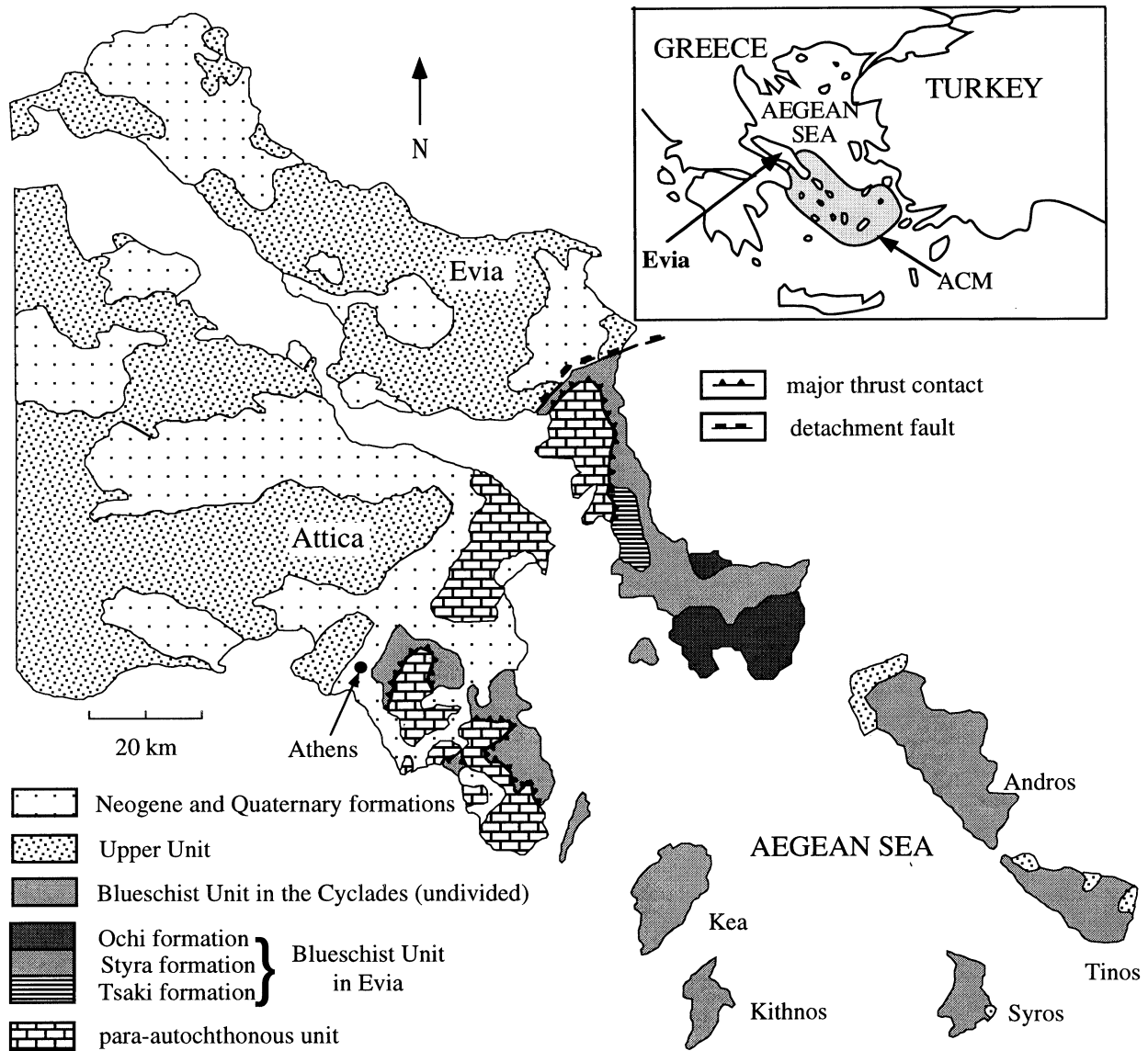


Fig. 1. A simplified geological map of the NW Cyclades, Evia and Attica, after Katsikatsos (1991) and Shaked *et al.* (2000), showing the tectonic contacts of the Blueschist Unit (subdivided in southern Evia) with rock sequences of the Hellenides. The Blueschist Unit is thrust over a para-autochthonous unit, the Almyropotamos Mesozoic platform, covered by an Eocene flysch, which was metamorphosed at pressures slightly lower than those of the Blueschist Unit (Shaked *et al.*, 2000). A low-angle normal fault (not shown in the NW Cyclades) separates the Blueschist Unit from the overlying Upper Unit (Avigad & Garfunkel, 1991), composed of the Pelagonian Unit in Evia, and of greenschist facies metamorphic sequences in the NW Cyclades. ACM, Attic-Cycladic Massif.

unparalleled in other Cycladic HP/LT rocks, makes them an ideal target for petrographic and geochemical study aimed at unravelling the tectono-magmatic province from which they were derived. It is necessary, however, to take into account the geochemical effects of oceanic hydrothermal alteration and later metasomatic processes expected during metamorphism of mélanges due to the close proximity of rocks of extremely different composition and water content.

2 Detailed petrological studies of the Cycladic eclogites in the last two decades showed similar peak P - T conditions along a north-east-trending 'eclogite axis'

from Sifnos towards Syros and Tinos (Okrusch & Bröcker, 1990). In order to draw at least a two-dimensional picture of the subducted plate, the metamorphic conditions of southern Evian outcrops, which lie perpendicular to this eclogite band, have to be accurately defined. In this respect, metabasic rocks, which abundantly occur in both southern Evia and NW Cyclades, are potentially the best recorders and preservers of HP/LT metamorphism.

3 Extension-related structures, including low-angle detachments juxtaposing low-grade rocks on top of exhumed eclogites and S - C fabrics overprinting

HP/LT assemblages in core complexes, have been widely described in the Cyclades and Evia (Lister *et al.*, 1984; Avigad & Garfunkel, 1989; Buick, 1991; Gautier & Brun, 1994). These indicate the onset of the Aegean back-arc extension as early as the Oligocene–Miocene boundary (Avigad *et al.*, 1997; Jolivet & Patriat, 1999). Much less is known, however, about tectonic processes responsible for the exhumation of the HP/LT rocks in the time interval between their creation at Cretaceous–Eocene times to overprinting at the Early Miocene (Altherr *et al.*, 1979; Maluski *et al.*, 1987; Bröcker & Enders, 1999). Southern Evia is a key area in studying the exhumation process, since here the allochthonous character of the Cycladic Blueschist Unit is best displayed, in the form of a basal thrust along which it was emplaced on top of lower pressure metamorphic sequences in Late Eocene–Oligocene times (Dubois & Bignot, 1979; Shaked *et al.*, 2000).

REGIONAL SETTING

The NW part of the Attic-Cycladic Massif, including southern Evia, is dominated by a thick Blueschist Unit (Fig. 1) derived from Mesozoic (Dürr *et al.*, 1978) carbonate, clastic and volcanic protoliths, probably representing a basic to intermediate volcanic province. The presence of some ophiolitic mélanges (Jacobshagen, 1986; Dixon & Ridley, 1987; Papanikolaou, 1987) shows that an oceanic basin constituted part of this province.

This Mesozoic sequence underwent a metamorphic history that includes an Eocene high- P/T event (M1), followed by a Late Oligocene–Early Miocene medium- P metamorphic overprint (M2) (Altherr *et al.*, 1979; Maluski *et al.*, 1987; Bröcker *et al.*, 1993). Recent U–Pb zircon studies show that high-pressure metamorphism commenced in the Upper Cretaceous (Bröcker & Enders, 1999). This M1 high- P/T event is well documented in southern Evia by $^{39}\text{Ar}/^{40}\text{Ar}$ dating of glaucophane and phengite, which gave ages of 50–45 Ma (Maluski *et al.*, 1981). Younger ages of 35–30 Ma were determined for phengite, but were attributed to partial resetting by the Miocene overprint (Schliestedt *et al.*, 1987). A decrease in M1 P – T conditions from 15 ± 3 kbar and 500 °C in Tinos, Syros and Sifnos eclogites (Central Eclogite Axis), north-westwards through epidote blueschists in Andros (10 kbar, 450 °C) to lawsonite blueschists in Evia (8 kbar, 300 °C), was postulated by Blake *et al.* (1981) and Bonneau & Kienast (1982). Lawsonite, pumpellyite and aegirine are considered to be part of the high-pressure paragenesis in southern Evia (Reinecke, 1986; after Bavay & Romain-Bavay, 1980), and M1 conditions were estimated at $T \leq 400$ °C and $P \geq 8$ kbar. More recently, Klein-Helmkamp *et al.* (1995) argued for peak pressures of 11 kbar, and Shaked *et al.* (2000) and Lensky *et al.* (1997) estimated minimum pressures of 10–12 kbar and temperatures of 380–450 °C. The

M2 overprint occurred throughout the NW Cyclades at greenschist facies conditions: $P = 4$ – 7 kbar and $T = 400$ – 500 °C (Reinecke, 1982; Matthews & Schliestedt, 1984; Avigad *et al.*, 1992; Bröcker *et al.*, 1993). On Evia, however, the M2 overprint of the high-pressure assemblages occurred within the stability field of pumpellyite at $T < 400$ °C (Reinecke, 1986; Lensky *et al.*, 1997).

TECTONO-STRATIGRAPHY OF THE BLUESCHIST UNIT IN SOUTHERN EVIA

The lower tectonic contact of the Cycladic Blueschist Unit is well exposed in southern Evia, where it overlies the para-autochthonous Almyropotamos Unit (Fig. 1), which consists of a thick series of metacarbonates and schists of Mesozoic to Eocene depositional age (Dürr *et al.*, 1978; Katsikatsos *et al.*, 1986). The Blueschist Unit in southern Evia consists of three formations, interpreted as imbricated nappes (Katsikatsos, 1991) (Fig. 2). From base to top they are as follows.

1 The Tsaki formation that consists mainly of pelitic lithologies with some impure marbles in its upper part. Close to the contact with the underlying Almyropotamos flysch it contains serpentinite bodies (up to several hundred metres in diameter) and metre-sized metagabbroic and metabasaltic lenses embedded in the metapelitic schists. This sequence is referred to as the ‘Tsaki ophiolitic mélange’.

2 The intermediate Styra formation is composed of a 1 km thick marble sequence with very thin horizons of quartzite, intercalations of metapelitic schist and rare blocks of metabasic rocks near its base.

3 The uppermost Ochi formation consists of a more than 1 km thick sequence of metasedimentary and metavolcanic rocks. The highest part of the Ochi formation, designated as the Kastri subunit by Jacobshagen (1986) (Fig. 2), is formed by a quartzite-rich sequence with horizons of metarhyolite and contains an ophiolitic mélange consisting of metabasic blocks within a serpentinite matrix (Lensky *et al.*, 1997).

The major ophiolitic mélange body occurs in the c. 300 m thick interval between the basal volcanogenic section of the Ochi Unit and the carbonate-rich intercalation of Kaki-Skala. This sequence is referred to as the ‘Ochi ophiolitic mélange’. The area surrounding the peak of Mt. Ochi, where the mélange is best exposed, were mapped in this work at a scale of 1:5000 (Fig. 3). An irregular body of metagabbro, up to a few hundred metres thick, is overlain by a thin lens of metawehrlite. Metre-sized blocks of metapillow basalt occur at the lower and upper contacts of the metawehrlite. The adjacent metasedimentary sequence contains horizons of piemontite-rich chert and fine-grained crossite–spessartine–stilpnomelane quartzite, the latter being interpreted as metamorphosed ferromanganese biochemical sediment and referred to as ‘meta-ironstone’. The meta-igneous bodies are elon-

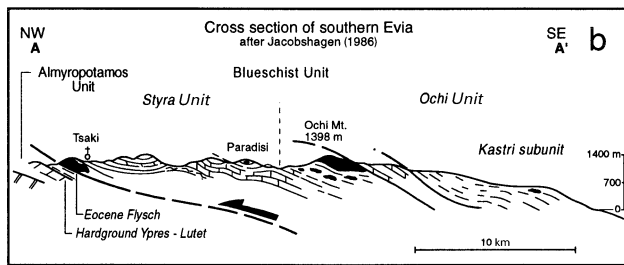
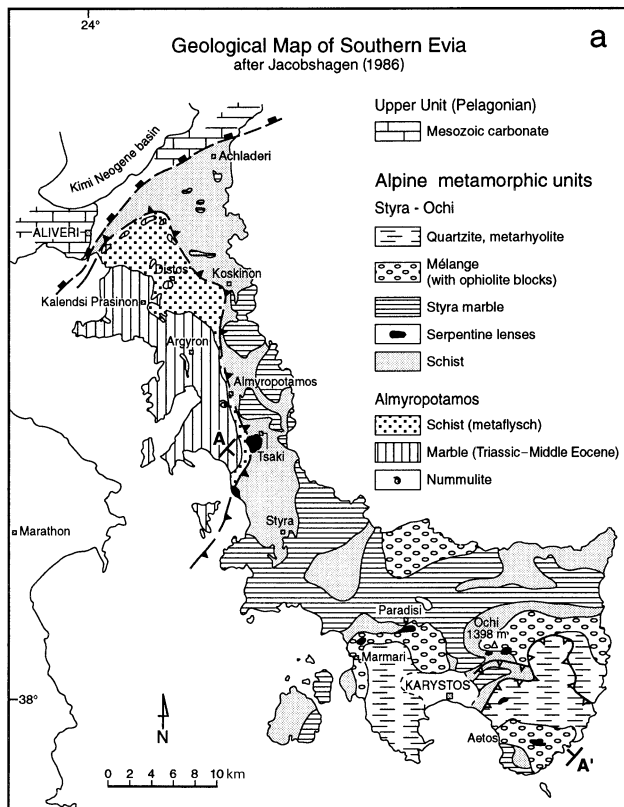


Fig. 2. Geological map (a) and cross-section (b) of southern Evia after Jacobshagen (1986) and Lensky *et al.* (1997), showing the tectonic contacts at the base and the top of the Blueschist Unit and interrelations among and within its formations. The peak of Mt. Ochi is shown in detail in Fig. 3.

gated parallel to the SW–NE strike of the dominant foliation, and to the glaucophane lineation in quartzites, ironstones and metagabbros. Metabasalt blocks occur at the wehrlite–gabbro contact and show that this section does not represent a continuous intrusive oceanic sequence. An original intrusive contact was found in the form of a metre thick ultrabasic dyke intruded into the gabbro (Figs 3 & 4a).

The ‘Ochi ophiolitic mélange’ is also exposed near the village of Paradisi (Fig. 2), where it is preserved in a synform. The lithology resembles that of the Mt. Ochi exposure: lens-shaped blocks of metawehrlite and metagabbro are embedded in the metaclastic country rocks, with some horizons of meta-ironstone. The

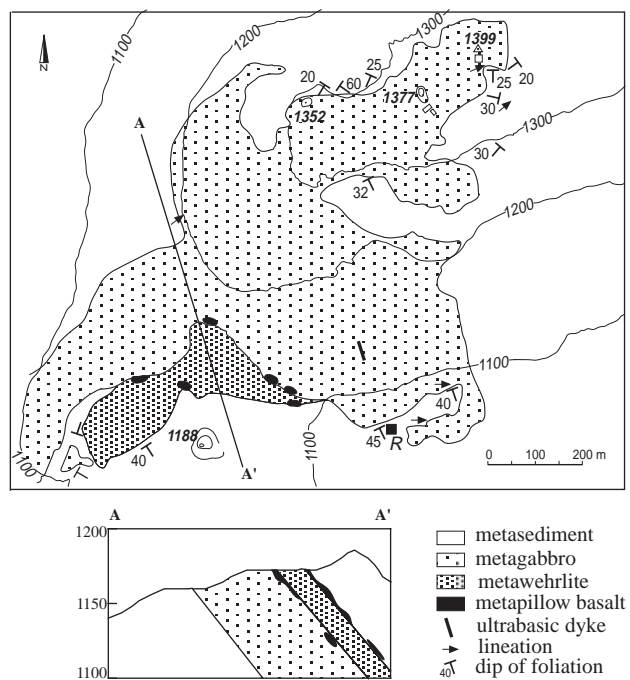


Fig. 3. Geological map and cross-section of the surroundings of the peak of Mt. Ochi (1399 m). *R*, Alpine refuge; open square, Hera temple; open rectangle, chapel.

blocks, however, are only several tens of metres in diameter.

ANALYTICAL METHODS

The mineral chemistry of representative rock samples was determined by a JEOL JXA 8600 electron microprobe. Electron beam conditions were 15 keV and 10 nA. The results were corrected by the ZAF method.

Major and 3d transition element contents were determined by inductively coupled plasma atomic emission spectrometry (ICP-AES), and rare earth element (REE) contents by inductively coupled plasma mass spectrometry (ICP-MS; Perkin Elmer, SCIEX Elan 6000). For major and trace element ICP analysis, rock powders were digested by melting with $\text{Li}_2\text{B}_2\text{O}_4$ in platinum crucibles and with Na_2O_2 in zirconia crucibles, respectively. Loss on ignition (LOI) was determined by heating the sample at 1050 °C for 4 h and correcting for the oxygen weight added by the oxidation of Fe^{2+} to Fe^{3+} .

The mineral and whole-rock oxygen isotope analyses were made with the laser fluorination extraction system at the Hebrew University of Jerusalem, which uses a Merchantek EO 30W CO_2 laser ablation station, BrF_5 reagent and a Micromass 602ES mass spectrometer. All analyses were corrected to the WJS quartz standard value $\delta^{18}\text{O} = 11.66\text{‰}$. The standard deviation of the quartz standard was $\pm 0.12\text{‰}$.

IGNEOUS AND METAMORPHIC EVOLUTION OF THE OPHIOLITIC MÉLANGES

The meta-igneous rocks of the Ochi and Tsaki ophiolitic mélanges occur near the top and at the bottom, respectively, of the Blueschist Unit. The mineralogy and petrography of these rocks define four major stages of crystallization comprising: (i) igneous crystallization during the formation of new oceanic lithosphere at a spreading centre; (ii) hydrothermal sea floor alteration; (iii) HP/LT metamor-

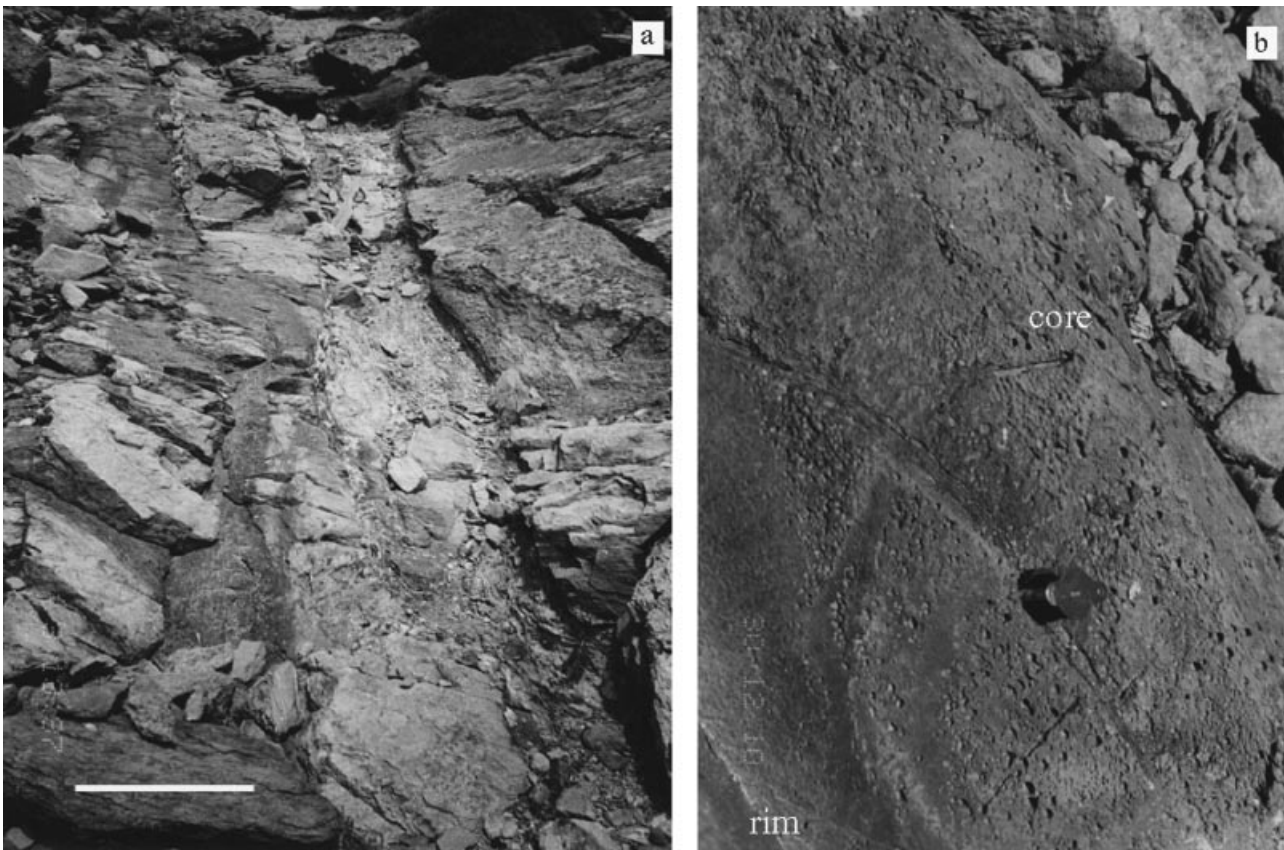


Fig. 4. Relict igneous features at Mt. Ochi exposure. (a) Meta-ultrabasic dyke cutting through metagabbro. The dyke consists of bright, highly sheared chlorite and tremolite metasomatic reaction zone. Scale bar, 1 m. (b) Core-rim variations in metapillow basalt: modal abundance of glaucophane (darker hue) decreases and abundance and size of vesicles increase from the pillow rim (lower left) to its core (upper right). A hand lens is shown for scale.

phism (M1); and (iv) a metamorphic overprint (M2) at pumpellyite-actinolite facies conditions. The main features of these crystallization stages are summarized in Table 1 and in the following descriptions.

Ochi ophiolitic mélange

Ultrabasic rocks

The ultrabasic rock of Ochi is a serpentinite characterized by poikiloblastic prismatic diopside which includes circular domains of serpentine, and is in turn enclosed within a serpentine matrix. The serpentines form a mesh texture commonly interpreted as a pseudomorphic texture of lizardite after olivine (Wicks & Whittaker, 1977). The presence of diopside, the relict poikilitic texture and the lack of pseudomorphic lizardite after orthopyroxene indicate that the ultrabasic rock was a cumulate wehrlite that underwent oceanic serpentinization. The diopside is commonly rimmed and sometimes almost completely replaced by brown titanian calcic amphibole (Fig. 5a), which is also partially serpentinized. The high alkali and Ti contents of the calcic amphibole (varying in composition from titanian edenite to titanian pargasite; Table 2, Fig. 6a,b) are consistent with an igneous origin.

The serpentinized igneous fabric is overgrown by a metamorphic assemblage that includes antigorite, diopside and tremolite. Diopside occurs either as a fan of fibres overgrowing serpentinitic mesh units or in continuous rims armouring igneous clinopyroxene ('shark teeth'; Fig. 5a,b). The neo-formed and relict igneous clinopyroxenes have similar Ca contents, but the igneous clinopyroxene tends to be

richer in Fe^{2+} , Al and Ti (Fig. 7). Antigorite overgrows the lizardite mesh texture (Fig. 5b). All serpentine minerals have anomalously high contents of FeO^* ($=\text{Fe}^{\text{total}}$ as Fe^{2+} ; 6–10 wt%) and Al_2O_3 (3–6 wt%) (Table 2), possibly reflecting higher availability of Fe and Al in a wehrlitic protolith, relative to other ophiolitic ultrabasic rocks (e.g. harzburgite).

Highly sheared (phylloitic) chlorite-tremolite 'blackwall', containing porphyroclasts of relict igneous amphibole, occurs at the contacts of the ultrabasic lens with the country rocks. The ultrabasic dyke that intruded the gabbro also has a phylloitic fabric. Relict porphyroclastic amphibole in this dyke (Fig. 6c,d) has cores of kaersutite or titanio sodic-calcic amphibole (barroisite to magnesio-katophorite) rimmed by bluish-green barroisite, and actinolite occurs at the outermost part of the crystals. The mineral chemistry of relict amphibole suggests that the dyke also originated as a wehrlite.

Metagabbroic rocks

The large metagabbroic body at Mt. Ochi is a porphyroclastically textured rock (flaser gabbro), containing large relict augite grains (up to 1 cm long) that are overgrown by glaucophane *sensu stricto* (Figs 5c & 8a) and enclosed in a well-oriented matrix of glaucophane, epidote, phengite (≤ 3.52 Si per formula unit (p.f.u.)), albite, chlorite, actinolite and pumpellyite (Fig. 9a). Glaucophane, epidote and phengite define the M1 assemblage and winchite occurs as a rare matrix mineral (Fig. 8c). Post-kinematic albite is dominant in the matrix, enclosing foliation-parallel inclusions of actinolite and epidote. Actinolite, chlorite, epidote, pumpellyite and phengite coexist in apparent textural equilibrium and define the M2 assemblage with albite.

Table 1. Mineral assemblages and textural characteristics of the igneous components of southern Evia ophiolitic mélanges classified according to four crystallization events: igneous formation, sea floor alteration and two regional metamorphic events.

		Ochi	Tsaki
Igneous	Ultrabasic	Cumulate wehrlite: Aug, Ti-amphibole Ultrabasic dyke: Ti-amphibole	Harzburgite (?) (pseudomorphs after Opx)
	Gabbro	Aug	
	Basalt	Pillowed, vesiculated, brecciated Aug	Massive, vesiculated Ti-augite (sub-ophitic)
Sea floor	Ultrabasic	Lz, Mag, Ilm	Lz, Mag, Ctl
	Gabbro	Paradisi: Hbl, Czo	Hbl, Czo
	Basalt	Core-to-rim zoning of the pillows. Py in pillow rims	Czo
M1	Ultrabasic	Di, Atg, Tr	Atg, Dol
	Gabbro	Mt. Ochi: Gln, winchite, Ep, phengite Paradisi: Omp (Jd ₄₁), Gln, winchite Ep, phengite, prograde lawsonite	Omp (Jd ₇₀), Gln, Ep, phengite Prograde lawsonite
	Basalt	Core: Omp (Jd ₅₃), phengite, Ep, Ab (veinlets) Rim fragments: Jd(Jd ₆₇)-Acm (Jd ₄₀), Qtz, ferroGln-Rbk, phengite (3.72) Rim matrix: ferroGln, Qtz, Ab	Jd(Jd ₈₇)-Omp(Jd ₂₄), Qtz, Gln-winchite
M2	Ultrabasic	Hem	
	Gabbro	Act, Pmp, Ep, Chl, Ab, phengite	Act, Pmp, Ep, Chl, Ab, phengite, Aug
	Basalt	Ep, Ab, Chl, phengite	Ep, Ab, Chl, Pmp, Bt

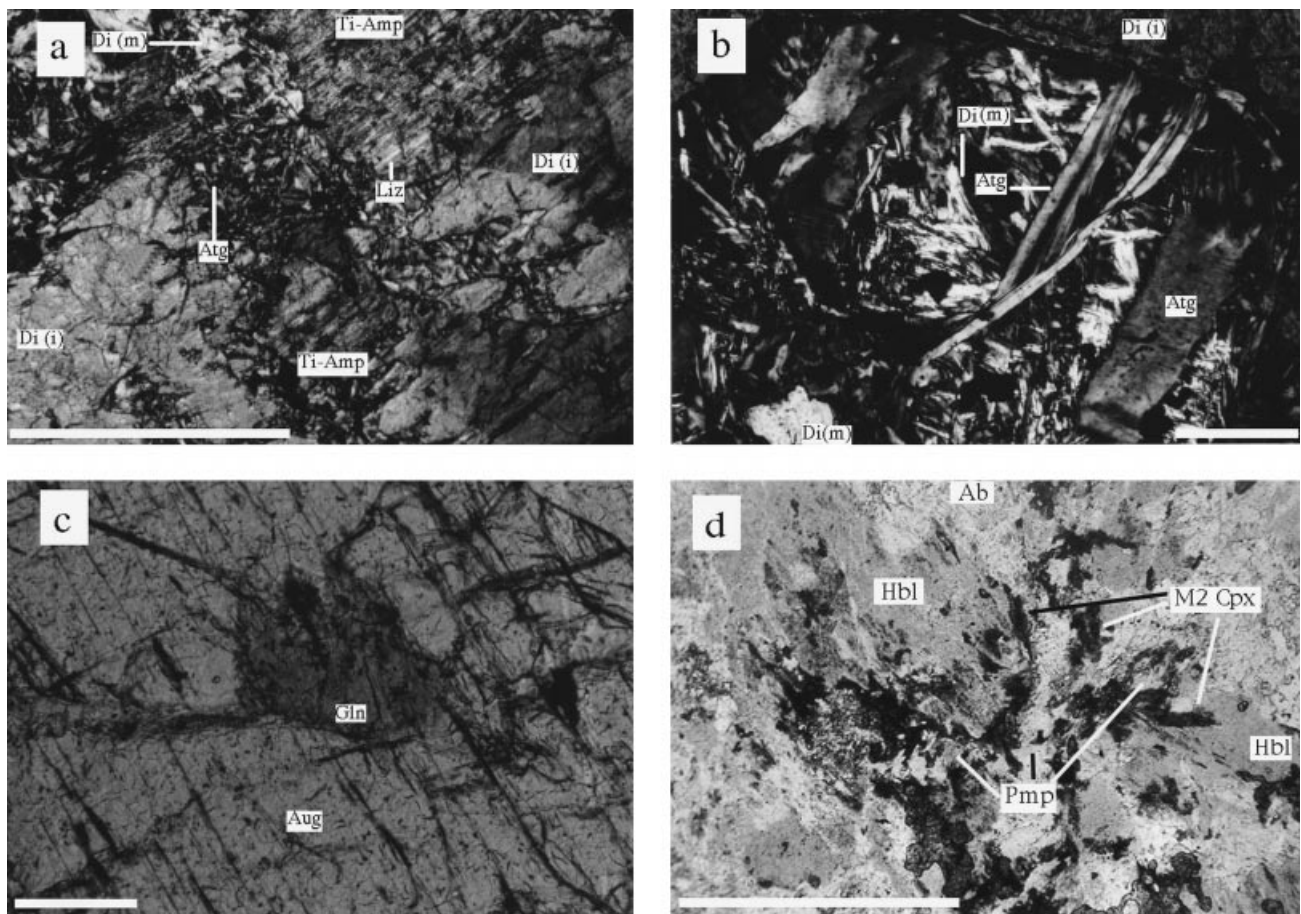
**Fig. 5.** Photomicrographs of thin sections from southern Evia ophiolitic mélanges. (a) Large crystals of igneous diopside are pseudomorphed at their margins by igneous Ti-amphibole, which is in turn serpentinized (bright bands within amphibole). The matrix consists of metamorphic diopside (bright) and antigorite (grey) overgrowing previous lizardite (dark background); Ochi metawehrlite (cross-polarized light, XPL). (b) Serpentine mesh unit after cumulate olivine enclosed within poikiloblast of igneous Cpx (dark margins of the photograph). Grey needles of antigorite and brighter diopside overgrow dark lizardite; Ochi metawehrlite (XPL). (c) Glaucophane patch (dark) overgrows igneous Cpx; Ochi metagabbro (plane-polarized light, PPL). (d) M2 assemblage of sodic augite (dark laths) and pumpellyite (bright grey patches) overgrows former oceanic hornblende (background); Tsaki metagabbro (PPL). Scale bars in photographs: (a, d), 1 mm; (b, c), 0.1 mm.

Table 2. Electron microprobe analyses of representative minerals from metabasic and meta-ultrabasic rocks of Ochi and Tsaki ophiolitic mélanges.

Sample (wt%)	1 Di	2 Di	3 Ed	4 Tr	5 Atg	6 Krs	7 Aug	8 Gln	9 Gln	10 Jd	11 Jd	12 Aug	13 Hbl	14 Atg
SiO ₂	52.17	55.55	45.69	56.74	37.73	43.66	50.04	56.94	56.18	56.78	57.44	53.05	48.69	40.98
TiO ₂	1.09	—	4.80	0.09	—	5.41	0.43	—	0.32	0.18	0.29	—	0.70	0.14
Al ₂ O ₃	3.02	0.18	8.62	0.50	6.65	10.51	4.53	11.01	7.56	12.86	18.16	1.51	8.19	1.85
Cr ₂ O ₃	0.77	0.17	1.09	0.61	—	—	0.11	—	—	—	—	—	—	0.28
FeO	4.05	2.12	6.33	4.01	8.06	7.68	5.15	8.94	16.04	11.58	4.94	9.36	11.34	3.16
MnO	0.12	—	—	0.00	0.15	0.11	—	—	0.22	—	—	0.13	0.33	0.10
MgO	14.94	16.67	15.24	21.91	32.84	14.77	15.77	10.69	6.92	1.19	2.06	11.80	14.35	42.79
CaO	22.41	24.31	10.85	12.45	—	11.21	23.25	1.69	0.84	2.29	3.89	22.19	12.07	—
Na ₂ O	0.34	0.33	3.39	0.71	—	3.22	0.18	6.64	6.63	12.38	12.00	1.26	1.77	—
K ₂ O	—	0.02	0.26	0.07	—	0.32	—	—	0.02	—	—	—	0.11	—
Sum	98.91	99.35	96.27	97.09	85.43	96.89	99.46	95.91	94.73	97.26	98.78	99.30	97.55	89.30
Cations														
Si	1.93	2.02	6.64	7.89	1.85	6.36	1.84	7.93	8.09	2.06	2.02	1.99	7.04	1.88
Ti	0.03	—	0.53	0.01	—	0.59	0.01	—	0.04	0.01	0.01	—	0.08	—
Al	0.13	0.01	1.48	0.08	0.38	1.80	0.20	1.81	1.28	0.55	0.75	0.07	1.40	0.10
Cr	0.02	0.01	0.13	0.07	—	—	—	—	—	—	—	—	—	0.01
Fe ³⁺	—	—	—	—	—	—	0.11	0.02	0.64	0.18	0.01	0.04	0.07	—
Fe ²⁺	0.13	0.07	0.77	0.47	0.33	0.94	0.05	1.03	1.29	0.17	0.14	0.25	1.30	0.12
Mn	—	—	—	—	—	0.01	—	—	0.03	—	—	—	0.04	—
Mg	0.82	0.91	3.30	4.54	2.40	3.21	0.86	2.22	1.49	0.06	0.11	0.66	3.09	2.93
Ca	0.89	0.95	1.69	1.86	—	1.75	0.92	0.25	0.13	0.09	0.15	0.89	1.87	—
Na	0.02	0.02	0.96	0.19	—	0.91	0.01	1.80	1.85	0.87	0.82	0.09	0.50	—
K	—	—	0.05	0.01	—	0.06	—	—	—	—	—	—	0.02	—
Sum	3.97	3.99	15.55	15.12	4.96	15.63	4.00	15.04	14.84	3.99	4.01	3.99	15.41	5.04

—, represents concentrations below the detection limit of the electron microprobe (<0.01 wt% or <0.01 cations p.f.u.). All Fe was assumed to be divalent in antigorite. Fe³⁺ in clinopyroxene was estimated by stoichiometry. Fe³⁺ in amphibole was estimated according to the method of Leake *et al.* (1997). Ochi metawehrlite: 1, Eor 75/37 igneous Cpx; 2, Eor 75/24 metamorphic Cpx; 3, Eor 75/28 igneous titanite-amphibole; 4, Eor 101/19 metamorphic tremolite; 5, Eor 75/18 antigorite; Ochi ultrabasic dyke: 6, Eor 140/21 relict kaersutite; Ochi metagabbro: 7, Eor 81/20 igneous augite; 8, Ep38/24 glaucophane; Ochi metabasalt: 9, Eor 103/12 glaucophane; 10, Eor103/21 jadeite; Tsaki metabasalt: 11, Et 54/37 jadeite; Tsaki metagabbro: 12, Et 48/13 M2 diopside; 13, Et48/38 relict hornblende; Tsaki serpentinite: 14, Et 115/1 antigorite.

The smaller metagabbro blocks that occur at the Paradisi exposure display several features additional to those observed at Mt. Ochi: (i) green hornblende pseudomorphs the igneous augite and in places is rimmed by actinolite (Fig. 8b), and rare inclusions of clinozoisite occur within epidote (Fig. 9b); both of these mineralogies are interpreted to reflect sea floor alteration; (ii) omphacite (Jd₄₁₋₁₆Aug₅₀₋₇₃Ac₉₋₁₁; Fig. 10a) overgrows augite or forms neoblasts in the matrix; (iii) tiny inclusions of lawsonite occur within albite and are associated with parallel-aligned inclusions of glaucophane and Si-rich phengite (up to 3.54 Si p.f.u.).

Metabasalts

The high-pressure (M1) mineralogy is best developed in the metabasaltic blocks of Mt. Ochi. The basalts are mostly pillowed with green, omphacite-rich cores mantled by blue, glaucophanitic rims (Fig. 4b). The exterior parts of the pillows are locally brecciated, forming angular Na-pyroxene-rich clasts in a glaucophane-rich matrix. Omphacite in pillow cores is commonly fine grained, encloses relict augite and is locally replaced by epidote. Coarser, idiomorphic omphacite (Jd₂₂₋₅₃Aug₇₀₋₄₆Ac₈₋₁; Fig. 10a) grows at the margins of albite veinlets, that cut across the foliation. The vein albite is thus in textural equilibrium with omphacite, suggesting that this paragenesis slightly post-dated the main phase of M1 metamorphism and deformation. Albite, chlorite and phengite (≤ 3.42 Si p.f.u.) are interstitial minerals and constitute the M2 assemblage. Ferro-glaucophane (Fig. 8a) is the major mineral of the pillow rims, and in the brecciated areas occurs in veins with albite and quartz. The breccia fragments consist of jadeitic pyroxene (Jd₅₉₋₆₇Aug₈₋₁₁Ac₃₃₋₂₂; Fig. 10a) clasts with quartz inclusions, ferro-glaucophane and interstitial phengite (≤ 3.72 Si p.f.u.) and albite. The sodic amphibole and pyroxene are zoned from Al-rich cores to Fe³⁺-rich rims (Figs 8a & 10a).

The basaltic blocks are cut by chlorite veins which are overgrown by pumpellyite and prismatic aggregates of clinozoisite and muscovite (Fig. 9a,b). Lensky *et al.* (1997) identified the latter at Aetos (Kastri subunit) as pseudomorphs after lawsonite and concluded that the

pumpellyite + lawsonite assemblage formed during syn- to post-M2 Ca-metasomatic alteration of chlorite.

Tsaki ophiolitic mélange

Ultrabasic rocks

The Tsaki ultrabasic rocks are serpentinites composed of interpenetrating antigorite blades (up to 0.4 mm in length) and minor dolomite. The low Al and Fe contents of the antigorite (Al₂O₃ = 1.85 wt%, FeO* = 3.16 wt%; Table 2) and the bastite texture consisting of plates of lizardite after orthopyroxene suggest that the protolith of the Tsaki serpentinite was a mantle harzburgite.

Metagabbroic rocks

The metagabbro consists of magnesiohornblende (Figs 5d & 8b) in a clinozoisite-rich matrix (Fig. 9c). This fabric was possibly acquired during intense sea floor uraltization and saussuritization of the gabbroic protolith. High-pressure (M1) metamorphism is manifested by the presence of numerous inclusions of omphacite (Jd₂₅₋₇₀Aug₇₂₋₃₀Ac₂₋₀; Fig. 10a) and of a few crystals of lawsonite within late albite, and the occurrence of pale-bluish patches of glaucophane (Fig. 8a) within coarse-grained calcic amphibole. In places, the M2 mineralogy dominates the fabric: epidote rims earlier clinozoisite (Fig. 10c) and coexists with pumpellyite (Fig. 10a) and actinolite, which replace earlier hornblende. Chlorite, albite, phengite (≤ 3.46 Si p.f.u.) and titanite are ubiquitous.

Unique to the Tsaki metagabbros compared with the other metabasites of the Blueschist Unit is the fan-shaped metamorphic diopside (Jd₁₀Aug₈₃Ac₇; Fig. 10a,b), statically overgrowing hornblende, and in textural equilibrium with pumpellyite and chlorite (Fig. 5d). This diopside has higher Fe²⁺ contents and very low Ti contents compared with the igneous augite (Fig. 10b-d). The texture and composition resemble the clinopyroxene formed during Sanbagawa metamorphism at pumpellyite-actinolite facies con-

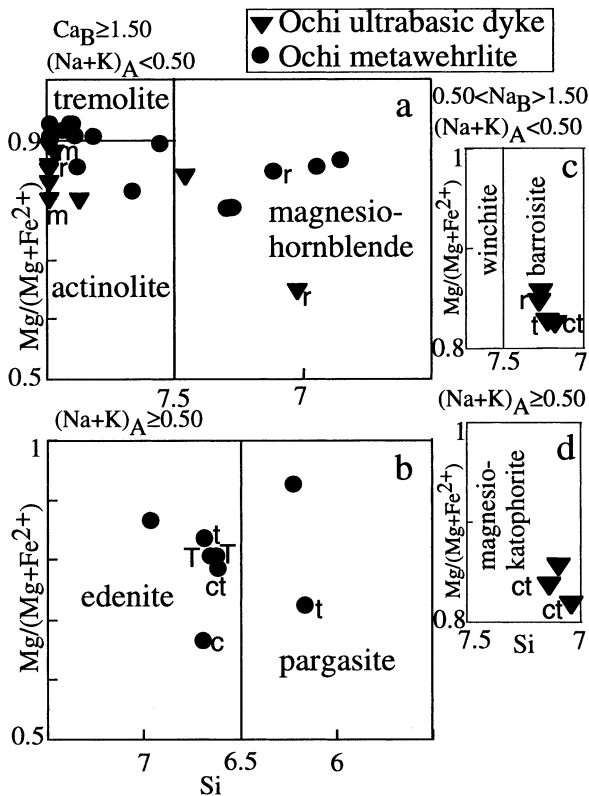


Fig. 6. Calcic amphibole (a, b) and sodic–calcic amphibole (c, d) compositions from Ochi meta-ultrabasic rocks, classified according to Leake *et al.* (1997); c, core; r, rim; m, margin; t, titanite amphibole ($0.25 < \text{Ti} < 0.49$); T, titanite amphibole ($\text{Ti} > 0.50$). Kaersutites ($\text{Ti} \geq 0.50$, $5.5 > \text{Si} < 6.5$; not shown here) also occur within Ochi ultrabasic dyke.

ditions (Maruyama & Liou, 1985). It is thus concluded that this diopside belongs to the M2 paragenesis.

Metabasalts

An igneous subophitic texture is well preserved in the Tsaki metabasalts in the form of fine-grained xenomorphic clinopyroxene partially included in albite. This igneous clinopyroxene is zoned from pinkish Ti-augite cores (Fig. 10b–d) to pale-greenish sodic pyroxene. The sodic pyroxene in these rocks is zoned from jadeitic cores ($\text{Jd}_{87-80}\text{Aug}_{13-19}\text{Ac}_{0-1}$) to omphacitic rims ($\text{Jd}_{24-50}\text{Aug}_{76-49}\text{Ac}_{0-1}$; Fig. 10a). Additional phases are clinozoisite rimmed by epidote and chlorite intergrown with minor green biotite and pumpellyite, representing the M2 assemblage. Vesicles occur, but in contrast with Ochi pillow basalts they are smaller (2–3 mm across), homogeneously distributed and filled with metamorphic minerals. Three different assemblages are observed within the vesicles: (i) prismatic clinozoisite containing inclusions of muscovite and calcite (by analogy with the Ochi rocks, these could represent pseudomorphs after lawsonite); (ii) aggregates of chlorite with minor relict glaucophane rimmed by winchite (Fig. 3); and (iii) rarely coexisting albite, omphacite and quartz.

PETROLOGY AND THERMOBAROMETRY

High-pressure (M1) metamorphism in metabasites

The abundant high-pressure epidote–glaucophane–omphacite paragenesis in the gabbroic and basaltic

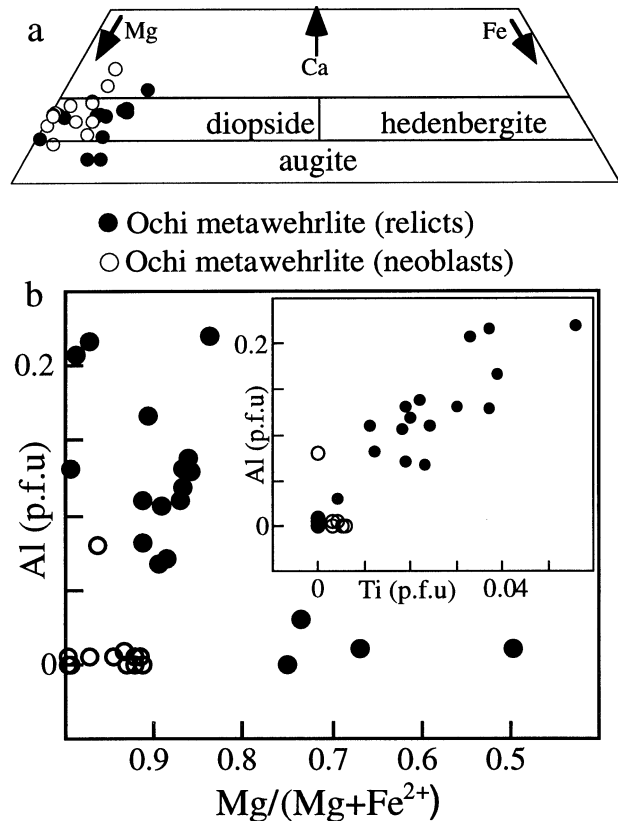


Fig. 7. (a) Clinopyroxene compositions from Ochi meta-ultrabasic rocks plotted on a section of the Mg–Ca–Fe triangle of Morimoto (1988). The long and short bases of the quadrilateral are $\text{Ca}/(\text{Ca} + \text{Mg} + \text{Fe}) = 0.4$ and 0.6 , respectively. (b) Al content (atoms per formula unit) versus Mg number and Ti content (atoms per formula unit) in clinopyroxene from Ochi meta-ultrabasic rocks. Note that very low Al and Ti contents are characteristic of metamorphic neoblasts.

rocks defines the grade of metamorphism as epidote–blueschist facies (Evans, 1990). Relict lawsonite enclosed in retrograde albite within Ochi (Paradisi exposure) and Tsaki metagabbros possibly records the earlier prograde P – T path within the lawsonite stability field. The replacement of omphacite by epidote in Ochi pillow cores is analogous to the breakdown of clinopyroxene to epidote + sodic amphibole observed in the Ward Creek metabasic exposure of the uppermost epidote zone of the Franciscan blueschists (Maruyama & Liou, 1987). The occurrence of winchite in Ochi metagabbros and Tsaki metabasalt is also indicative of equilibration at the uppermost epidote zone, above the actinolite–glaucophane solvus (Liou & Maruyama, 1987).

The M1 P – T conditions of the Ochi and Tsaki metabasites are partially constrained by the petrogenetic grid for epidote blueschists calculated by Evans (1990). This grid is plotted in Fig. 11 using the sodic amphibole composition 2 of Evans (1990), which is close to that of Evia glaucophane. The grid places temperature limits of $350 \leq T \leq 520$ °C for the epidote–

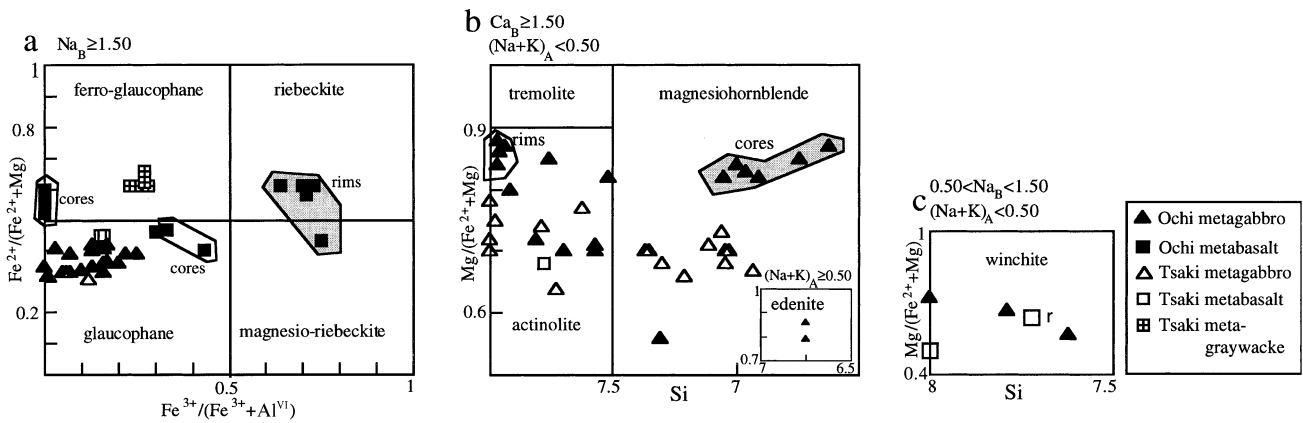


Fig. 8. Sodic amphibole (a), calcic amphibole (b) and sodic-calcic amphibole (c) compositions from Ochi and Tsaki metabasic rocks, classified according to Leake *et al.* (1997). Winchite rims (r) glaucophane in Tsaki metagabbro.

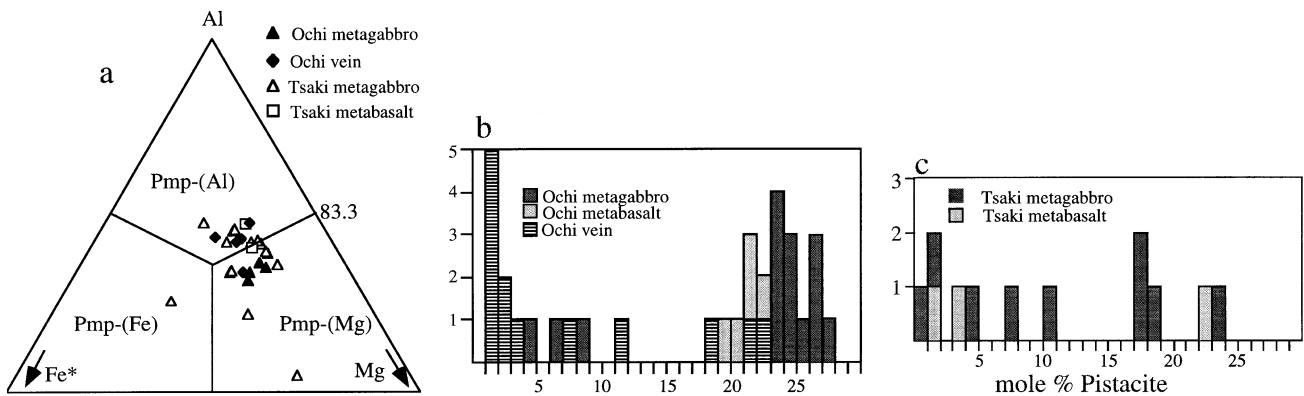


Fig. 9. Ca–Al silicate compositions from Ochi and Tsaki metabasic rocks and from veins cutting metabasalts in Ochi. (a) Pumpellyite compositions plotted on a section of the Fe^* (total Fe as Fe^{2+})–Al–Mg triangle and classified according to Coombs *et al.* (1976). Epidote compositions distributed according to molar per cent pistacite in Ochi (b) and Tsaki (c).

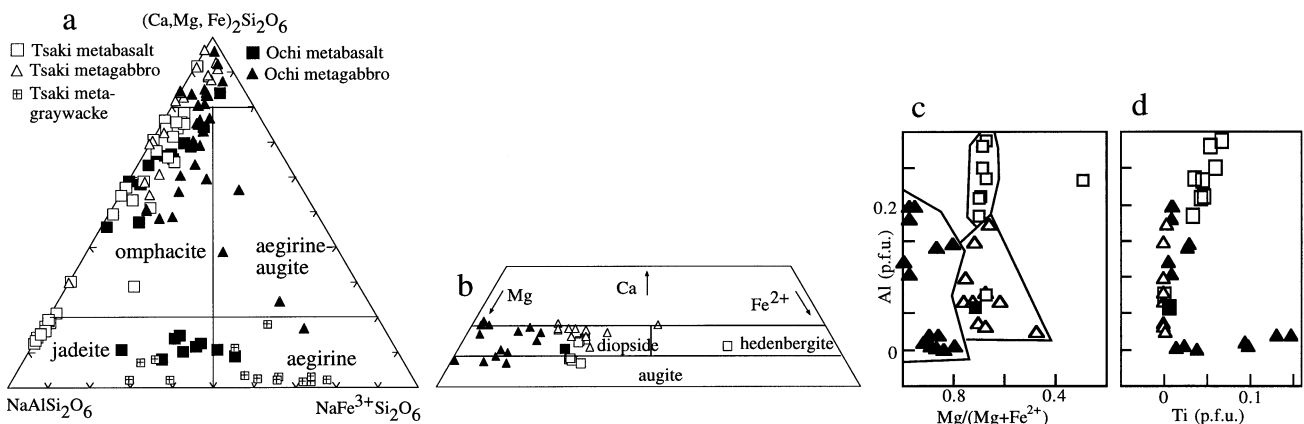


Fig. 10. Clinopyroxene compositions from Ochi and Tsaki metabasic rocks. (a) Na–Ca-pyroxene and Na-pyroxene plotted on the Aug–Jd–Ac triangle of Morimoto (1988). (b) Ca–Mg–Fe ‘quadrilateral’ pyroxene plotted on a section of the Mg–Ca–Fe triangle of Morimoto (1988) (see Fig. 7a). (c, d) Compositional grouping of clinopyroxene on Al content (p.f.u.) versus Mg number and Ti content (p.f.u.) diagrams. Note that very low Al and Ti contents are characteristic of M2 metamorphic augite from Tsaki.

blueschist assemblage. The upper temperature limit of *c.* 500–530 °C given by the *P–T* grid is considered to be too high for the Evian M1 event. For example, garnet is not found in the metabasalts and metagabbros

of the Mt. Ochi exposure, whereas 460 °C epidote–blueschist metabasites of similar bulk chemical composition in the Seward Peninsula, Alaska, have abundant almandine-rich garnet (Patrick & Evans, 1989).

Mn-rich garnet is formed in the Kastri subunit metabasalts (Lensky *et al.*, 1997). The lower stability of garnet in blueschists is defined by the reaction in the haplobasaltic system: $19\text{Chl} + 38\text{Qtz} + 4\text{Czo} = 25\text{Prp} + 4\text{Tr} + 74\text{H}_2\text{O}$ (Evans, 1990). The univariant line calculated using the Thermocalc 2.5 code (Holland & Powell, 1998) for Kastri garnet ($X_{\text{Prp}} = 0.02$) and the mineral component activities of Kastri metabasites plot at 433 °C, 8 kbar and 408 °C, 14 kbar (Fig. 11). An independent estimate of M1 temperatures is obtained from oxygen isotope thermometry of a metasedimentary ironstone from the Mt. Ochi area (Eor 67). Quartz and glaucophane separates from this rock gave $\delta^{18}\text{O}$ values of 16.57‰ and 12.01‰, respectively (Table 3). The quartz–glaucophane fractionation is determined by combining the experimental quartz–garnet fractionation of Rosenbaum & Matthey (1995) with the glaucophane–garnet equation, $1000 \times$

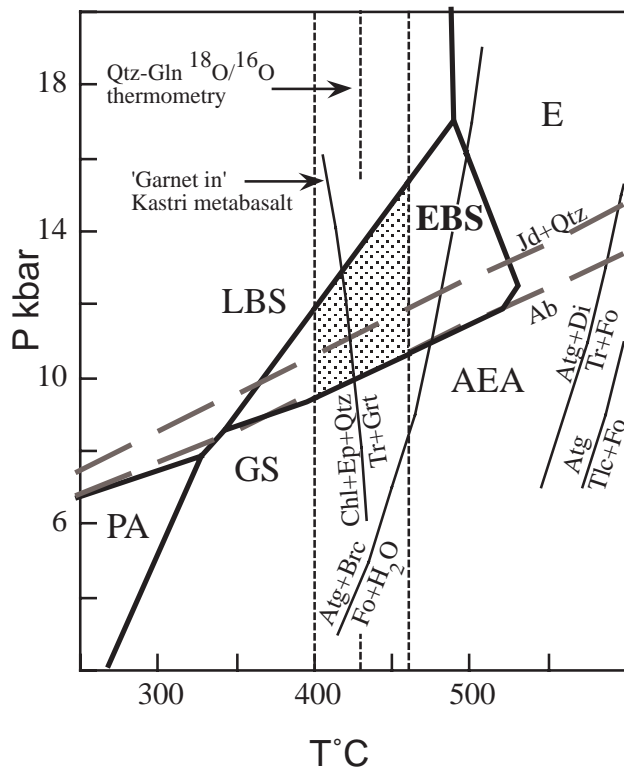


Fig. 11. Calculated T - $P_{\text{H}_2\text{O}}$ equilibria for M1 basic and ultrabasic assemblages in Ochi and Tsaki ophiolitic mélanges plotted on Evans (1990) petrogenetic grid for epidote blueschists in the NCMASH system (sodic amphibole composition no. 2). M1 conditions for Evia rocks are shown as a stippled region limited by the boundaries of the epidote-blueschist stability field (thick black line), $\text{Ab} = \text{Jd}^{\text{Cpx}} + \text{Qtz}$ reaction lines (thick broken grey line) and one standard deviation of Qtz–Gln stable isotope thermometry (thin broken lines). Note that the ‘garnet-in’ reaction calculated for Kastri metabasalt plots within the stippled region. Calculations were made using the software Thermocalc version 2.5 (Holland & Powell, 1998). AEA, albite epidote amphibolite; E, eclogite; EBS, epidote blueschist; GS, greenschist; LBS, lawsonite blueschist; PA, pumpellyite–actinolite.

Table 3. Laser probe oxygen isotope analyses of mineral separates from quartzites, metabasalts and metagabbros of southern Evia ophiolitic mélanges.

Sample	Rock type	Mineral	$\delta^{18}\text{O}$
Eor 67	Quartzite Ochi	Gln	12.01
		Qtz	16.57
Eor 106	Metabasalt Ochi	Gln	12.15
		Omp	9.60
Eor 17	Metagabbro Ochi	Ep	9.88
		Chl	9.83
		Aug	6.44
		Aug	6.40
		Aug	6.02
Eor 61	Metagabbro Ochi	Ep	11.17
		Act	11.08
		Act	10.44
Eor 70	Metagabbro Ochi	Gln	9.02
		Gln	8.71
Eok 1	Metagabbro Ochi	Gln	10.25
		Gln	10.61
Eok 81	Metagabbro Ochi	Aug	5.71
		Aug	5.62
		Aug	5.90
		Aug	5.44
		Aug	5.22
Ep 33	Metagabbro Paradisi	Hbl	9.22
		Hbl	6.61
		Chl	6.23
Ep 38	Metagabbro Paradisi	Omp	8.93
		Omp	9.67
Et 47	Metagabbro Tsaki	Hbl	12.70
		Hbl	12.36
Et 48	Metagabbro Tsaki	Pmp	13.03
		Hbl	13.17
		Hbl	13.14

$\ln \alpha_{\text{Gln-Grt}} = (0.87 \pm 0.15) \times 10^6 T^{-2}$, of Putlitz *et al.* (2000). The resulting equation, $1000 \times \ln \alpha_{\text{Qtz-Gln}} = 2.25 \times 10^6 T^{-2}$, yields a temperature of 430 ± 30 °C for the quartz–glaucophane pair in sample Eor 67. Based on the above considerations, it appears that a maximum temperature of about 450 °C would be appropriate for the M1 metamorphism.

Pressures within the epidote–blueschist field are constrained by the reaction $\text{Ab} = \text{Jd}_{\text{Cpx}} + \text{Qtz}$. The P - T conditions of this reaction were calculated for pyroxene showing the maximum jadeite contents in Mt. Ochi ($\text{Jd}_{0.67}$, in pillow rim Eor 103) and in Tsaki ($\text{Jd}_{0.87}$, in metabasalt Et 54) metabasites. At an estimated temperature of 450 °C, the calculated pressures are 10.4 and 11.5 kbar, respectively. These are considered minimum pressures, since apart from post-peak M1 albite–omphacite ($\text{Jd}_{0.53}$) veins in Ochi pillow cores, albite mostly replaces omphacite and the reaction occurs during the retrograde part of the P - T path. The difference in jadeite contents and calculated pressures may reflect higher $\text{Fe}^{3+}/\text{Fe}^{2+}$ in Ochi pillow rims, resulting in a higher acmite content in the sodic pyroxene (Fig. 10a). The silica in phengite barometer of Massonne & Schreyer (1987) gives pressures ranging from 10.5 to 14 kbar at 450 °C when applied to the phengite of the Blueschist Unit (maximum Si contents: 3.55 and 3.42 Si p.f.u. in Ochi metagabbros and pillow cores, respectively, and 3.46 in Tsaki metagabbro).

However, this estimate may not be well constrained since the barometer was calibrated for an assemblage which included K-feldspar, biotite and quartz, whereas phengite of the Evia blueschists equilibrated with other minerals, mainly Mg/Fe silicates. Consequently, the celadonite component in white mica is not fully buffered.

M2 metamorphism in metabasites

The M2 assemblage of metabasic rocks is Act–Pmp–Ep–Chl–Ab–phengite. This assemblage is characteristic of the pumpellyite–actinolite facies (Coombes *et al.*, 1976; Nakajima *et al.*, 1977; Liou *et al.*, 1987). Maximum temperatures for this paragenesis in the haplobasaltic system are given by the reaction, $25\text{Pmp} + 2\text{Chl} + 29\text{Qtz} = 7\text{Tr} + 43\text{Czo} + 67\text{H}_2\text{O}$ (Banno, 1998), which separates the pumpellyite–actinolite facies P – T field from that of the greenschist facies. The absence of lawsonite defines a lower temperature limit for this paragenesis according to the reaction: $5\text{Pmp} + 141\text{Lws} = 17\text{Czo} + \text{Chl} + 4\text{Qtz} + 33\text{H}_2\text{O}$ (Banno, 1998). The P – T conditions of these reactions calculated for the mineral compositions of Tsaki and Ochi metagabbros are shown in Fig. 12. At maximum pressures of 6–8 kbar (inferred from the absence of glaucophane from the M2 assemblages), these reactions define M2 temperature ranges of 300–350 °C and 290–330 °C at Tsaki and Ochi exposures, respectively.

The occurrence of sodic augite in the M2 assemblage of Tsaki metagabbros distinguishes it from the clinopyroxene-free M2 assemblage of Ochi metabasites. The presence of such sodic augite within pumpellyite–actinolite facies metabasites was studied in greenstones of the Mikabu complex, Sanbagawa belt, Japan by Maruyama & Liou (1985). They suggested that it formed by the reaction $\text{Pmp} + \text{Act} + \text{H}_2\text{O} = \text{Cpx} + \text{Chl} + \text{Qtz}$, and deduced that pyroxene–chlorite assemblages are stable at lower temperatures than those of pumpellyite–actinolite. A petrogenetic grid for the pumpellyite–actinolite facies in the Na_2O – CaO – MgO – Al_2O_3 – SiO_2 – H_2O (NCMASH) system was recently calculated by Banno (1998). This grid calculated using Thermocalc 2.5 for the Mg–Al–end-member phases Lws, Czo, Pmp, Di, Tr and Gln with clinocllore, Ab, Qtz and H_2O in excess is shown in Fig. 12. The grid shows that the Tsaki pumpellyite–diopside (PD) assemblage developed at lower temperatures than the pumpellyite–actinolite (PA) assemblage of Mt. Ochi metabasites. The low water activity of Mt. Ochi rocks relative to Tsaki could also account for the different assemblages. However, the presence of hydrated phases in M2 veins within the Mt. Ochi metabasites suggests that this alternative is unlikely.

Meta-ultrabasic rocks

The metamorphic assemblages that document the peak temperatures at Ochi and Tsaki meta-ultrabasic rocks

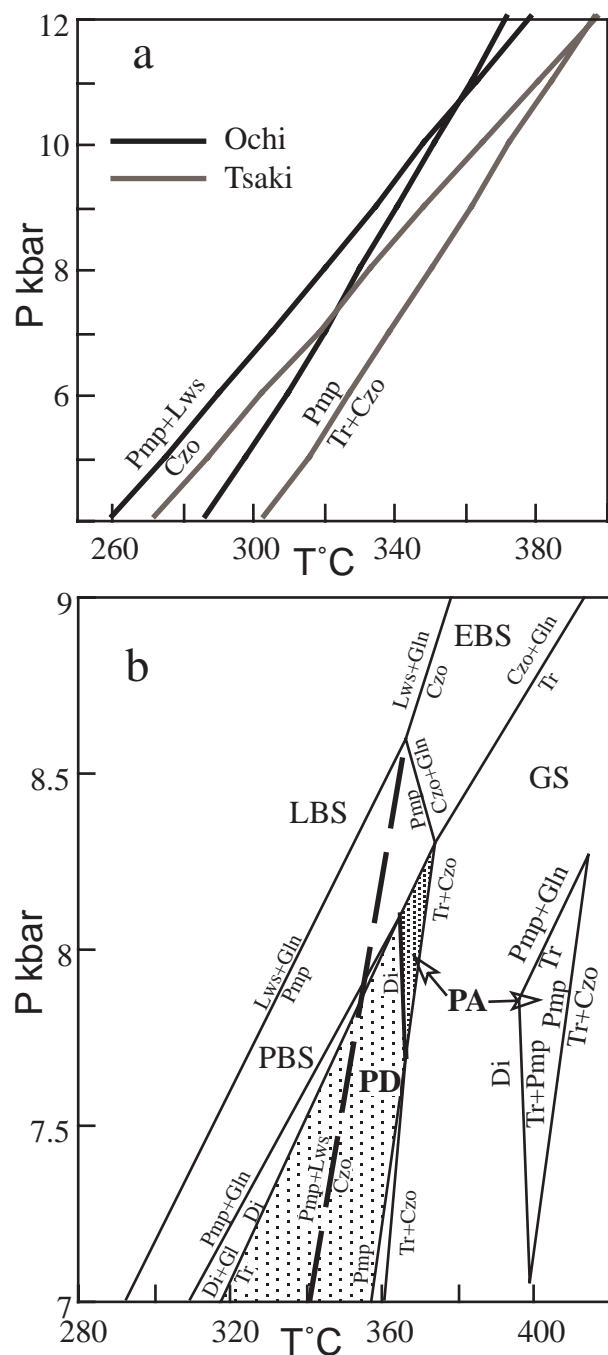


Fig. 12. (a) Univariant lines for the reactions, $25\text{Pmp} + 2\text{Chl} + 29\text{Qtz} = 7\text{Tr} + 43\text{Czo} + 67\text{H}_2\text{O}$ and $5\text{Pmp} + 141\text{Lws} = 17\text{Czo} + \text{Chl} + 4\text{Qtz} + 33\text{H}_2\text{O}$, calculated for mineral compositions of Ochi and Tsaki metagabbros. (b) Calculated P – T grid in the NCMASH system for the phases Lws, Czo, Pmp, Di, Tr and Gln with excess of clinocllore, Ab, Qtz and H_2O , showing stability fields for pumpellyite–diopside (PD) and pumpellyite–actinolite (PA) assemblages. Calculations were made using the Thermocalc software version 2.5 (Holland & Powell, 1998). PBS, pumpellyite blueschist; for other facies abbreviations, see Fig. 11.

are Atg–Di–Tr in Ochi metawehrlite and antigorite in Tsaki metaserpentinite. Since M1 temperatures are higher than those of M2, it is considered that these assemblages formed during the M1 metamorphic event. The high-temperature limit for the Ochi metawehrlite assemblage is given by the reaction: $\text{Atg} + 8\text{Di} = 4\text{Tr} + 18\text{Fo} + 27\text{H}_2\text{O}$ (Evans, 1977). This reaction is shown in Fig. 11, and at pressures of 9–11 kbar limits the coexistence of Atg+Di in Ochi wehrlites to maximum temperatures of 561–575 °C. The upper temperature limit in Tsaki serpentinites is defined by the absence of olivine, which is thought to form in such Mg-rich rocks by the reaction: $\text{Atg} + 20\text{Brc} = 34\text{Fo} + 51\text{H}_2\text{O}$ (Frost, 1975; Evans, 1977; Pinsent & Hirst, 1977). At pressures of 9–11 kbar, this reaction occurs at temperatures of 464–475 °C (Fig. 11). Brucite was not identified in the Tsaki serpentinites; however, given its expected relative paucity in recrystallized serpentinitized harzburgites, it may not be observed either visually or by X-ray powder diffraction (O'Hanley, 1996).

The petrogenesis and geothermobarometry of the HP/LT rocks in southern Evia thus indicate that their exhumation path involved cooling during decompression from epidote–blueschist facies conditions (T_{max} c. 450 °C; $P_{\text{min}} = 11$ kbar) to pumpellyite–actinolite facies conditions ($T_{\text{max}} = 350$ °C; $P_{\text{max}} = 8$ kbar).

GEOCHEMICAL EVOLUTION OF THE OPHIOLITIC MÉLANGES

Major and trace element composition

These studies were made in order to define the source and geochemical provenance of the igneous blocks. Representative major and trace element analyses of the metabasites and meta-ultrabasic rocks are listed in Table 4.

Mt. Ochi ophiolitic mélange

The SiO_2 contents (46–55 wt%) of metagabbros overlap with those of the metapillow basalts. The Mg numbers ($X_{\text{Mg}} = \text{Mg}/(\text{Fe} + \text{Mg})$ atomic ratio) of the two rock types are, however, different, varying from 0.31 to 0.59 in the pillows and from 0.58 to 0.76 in the metagabbros. The alkali element contents ($\text{Na}_2\text{O} + \text{K}_2\text{O}$) range from 4.5 to 7.3 wt% in the metagabbros and from 6 to 8 wt% in the metabasalts, and are much higher than the c. 2 wt% found in MORB (e.g. Stakes *et al.*, 1984). CaO contents are highly variable, ranging from 3.5 to 8 wt% in metabasalts and 1.5 to 9.5 wt% in the metagabbros, and are extremely low relative to the 12–13 wt% CaO contents typical of MORB. Alkali and Fe enrichment and Ca depletion relative to MORB are consistent with hydrothermal sub-sea floor alteration at an oceanic spreading centre (e.g. Ito & Anderson, 1983;

Thompson, 1983). Na and Fe enrichments are especially pronounced in the pillow rims (compare sample Eor 147 with Eor 103, 107; Table 4) and are reflected in the metamorphic rocks by the higher modal abundance of glaucophane. These, and the occurrence of pyrite, suggest that pillow rims were the rocks most affected by sea floor hydrothermal activity.

The Ochi metagabbros and metawehrlites show positive correlations on variation diagrams of the compatible elements Ni and Cr versus X_{Mg} (Fig. 13). These correlations are consistent with fractional crystallization in which the wehrlites (and probably also Paradisi gabbro Ep 33) formed as cumulates in a primitive magma, generating evolved magmas represented by most of the Ochi gabbros. The enrichment in Ni is also consistent with the poikilitic texture of the metawehrlites, which indicates early precipitation of olivine from the magma.

The REE are considered to be immobile during hydrothermal alteration and low-grade metamorphism (Michard, 1989). Ochi gabbros and basalts are well distinguished by their chondrite-normalized REE patterns (Fig. 14). Ochi metabasalts are highly fractionated and light rare earth element (LREE) enriched: the La content is up to 120 times chondrite values and $(\text{La}/\text{Yb})_{\text{CN}}$ values range from 5 to 10. These features indicate an enriched mantle source for Ochi basalts and are comparable with those of E-type MORB (Sun & McDonough, 1989). The Ochi metagabbros, however, show mildly LREE-enriched patterns ($(\text{La}/\text{Yb})_{\text{N}} = 2\text{--}3$, $\text{La} \leq 30$ times chondrite values). There are two possible explanations for the REE differences between the Ochi basalts and gabbros: (i) the mélange blocks were assembled from a heterogeneous source terrane, the gabbros having been formed in a less-enriched magmatic province (T-type MORB, supra-subduction zone (SSZ) setting); (ii) the depletion in incompatible elements in gabbros relative to basalts was due to the loss of residual melt by compaction.

The Ochi metabasalts and metagabbros show lower high field strength element (HFSE: Ce, P, Zr, Sm, Ti, Y) abundances relative to the large ion lithophile elements (LILE: Sr, K, Rb, Ba) on MORB-normalized incompatible element diagrams (spider diagram of Pearce, 1983; Fig. 15). A distinctive feature of all samples is a marked negative Nb anomaly: $(\text{La}/\text{Nb})_{\text{CN}} = 1.7$. Such patterns are characteristic of island arc tholeiites (IAT; Pearce, 1983) and back arc basin basalts (BABB; Saunders & Tarney, 1984; Monnier *et al.*, 1995), where melts are generated in a mantle affected by advective subduction zone fluids (e.g. Hawkesworth *et al.*, 1993). The patterns thus suggest that the igneous constituents of the Ochi ophiolitic mélange were derived from an SSZ environment rather than from a mid-oceanic ridge. The occurrence of wehrlites rather than other cumulates (Pearce *et al.*, 1984) in the mélange confirms the SSZ origin of Ochi ophiolites. An SSZ origin was also deduced for metabasites of the Blueschist Unit in

Table 4. Representative major, trace and rare earth element (REE) analyses of metabasites and meta-ultrabasic rocks from southern Evia ophiolitic mélanges.

(a) Ochi ophiolitic mélange.

wt%	Eok 1	Eor 10	Ep 33	Ep 38	Em 123	Eor 103	Eor 107	Eor 147	Eor 171	Ep 40	Eok 8	Eor 75
SiO ₂	46.9	51.3	45.8	54.4	50.5	62.8	52.4	53.7	45.8	39.1	39.3	37.6
Al ₂ O ₃	13.60	15.04	11.60	16.04	17.10	9.94	11.66	17.81	17.60	5.76	6.62	6.15
Fe ₂ O ₃	13.10	8.68	10.17	7.30	8.38	13.15	17.68	7.14	12.08	12.40	10.83	13.25
TiO ₂	2.76	1.15	1.06	1.18	1.42	0.37	0.47	1.07	1.54	0.45	0.42	0.50
CaO	4.72	7.71	7.14	3.41	4.26	1.64	3.75	4.06	9.01	3.91	3.55	2.46
MgO	8.98	6.89	16.50	7.27	7.37	3.04	4.23	5.09	4.27	28.10	29.0	28.3
MnO	0.36	0.16	0.16	0.10	0.10	0.11	0.39	0.17	0.20	0.16	0.19	0.17
Na ₂ O	4.45	4.59	2.31	6.44	3.76	7.65	6.16	5.53	5.87	0.11	0.16	0.11
K ₂ O	0.11	1.24	0.09	0.60	2.76	0.13	1.51	2.08	0.26	0.05	0.07	0.04
P ₂ O ₅	0.4	0.2	0.1	0.3	0.4	0.3	0.1	<0.1	0.1	<0.1	0.1	0.1
LOI	3.60	2.84	4.70	2.54	4.14	1.03	1.74	2.96	2.83	9.38	9.84	10.60
Total	98.98	99.80	99.63	99.58	100.19	100.16	100.09	99.61	99.56	99.42	100.08	99.28
ppm												
Ba	23	315	38	105	363	24	230	595	35	10	18	17
Cr	117	267	820	134	163	52	70	108	66	1760	2470	2230
Nb	6.3	1.4	2.2	5.6	6.2	5.0	6.3	7.0	11.0	1.0	1.0	0.9
Ni	31	96	510	67	76	76	131	62	108	1060	1485	1540
Rb	2	18	1	8	34	2	38	38	8	2	1	1
Sr	105	462	107	208	500	46	292	416	110	190	42	20
Ta	0.8	0.2	0.3	0.5	0.6	0.7	0.8	0.8	1.1	0.2	0.5	0.3
Th	1.4	0.6	0.8	1.0	0.9	6.0	6.0	7.5	4.8	0.6	0.8	0.2
Y	40	16	17	23	24	33	26	32	28	9	10	11
										C1		
La	11	5	5	9	11	37	38	24	27	0.31		
Ce	31	13	11	24	26	40	49	50	50	0.808		
Pr	5.0	2.0	1.7	3.4	3.8	8.8	8.4	6.7	7.7	0.122		
Nd	24	9.3	8.2	15.7	17.5	36	33	28	33	0.6		
Sm	6.4	2.4	2.2	3.8	4.0	8.0	6.4	6.3	7.2	0.195		
Eu	2.0	0.8	0.8	1.3	1.4	1.5	1.3	1.7	2.0	0.074		
Gd	5.5	2.0	2.1	3.3	3.4	5.9	5.0	4.8	5.3	0.259		
Tb	1.1	0.4	0.4	0.6	0.6	1.0	0.8	0.8	0.8	0.047		
Dy	6.6	2.6	2.7	3.7	4.0	6.0	4.5	5.1	4.9	0.322		
Ho	1.3	0.5	0.6	0.8	0.8	1.2	0.9	1.1	1.0	0.072		
Er	3.9	1.6	1.6	2.3	2.4	2.6	3.3	3.3	2.9	0.21		
Tm	0.5	0.2	0.2	0.3	0.3	0.5	0.4	0.5	0.4	0.032		
Yb	3.4	1.5	1.5	2.1	2.3	3.3	2.4	3.5	2.9	0.209		
Lu	0.5	0.2	0.2	0.3	0.4	0.5	0.4	0.6	0.4	0.032		

Major and trace elements measured by inductively coupled plasma atomic emission spectrometry (ICP-AES) analysis. REE measured by inductively coupled plasma mass spectrometry (ICP-MS). Eok 1, Eor 10, Ochi metagabbro; Ep 33, Ep 38, Em 123, Paradisi metagabbro; Eor 103, Eor 107, Ochi pillow rims; Eor 147, Eor171, Ochi pillow cores; Ep 40, Paradisi metawehrlite; Eok 8, Eor 75, Ochi metawehrlite; C1, chondrite composition from Boynton (1984). (b) Tsaki ophiolitic mélange.

adjacent NW Cycladic islands (Bröcker, 1991; Seck *et al.*, 1996).

Tsaki ophiolitic mélange

The MgO, Ni and Cr contents of Tsaki serpentinite are higher than those of Ochi metawehrlite (Table 4, Fig. 13), and are consistent with a mantle origin. The Al₂O₃ content (1.5 wt%) corresponds to that of harzburgite. Metabasalts are moderately enriched in alkalis and depleted in Ca relative to MORB (4.6 & 5–9 wt%, respectively), indicating a similar degree of spilitization to that observed in Ochi metagabbros. The Ca and Na contents of Tsaki metagabbros are similar to those of MORB. In contrast to the highly LREE-enriched patterns of Ochi metabasites, the Tsaki metagabbros display almost unfractionated REE patterns, with a slight depletion in LREE [(La/Yb)_N = 0.7; Fig. 14], that are similar to those of N-MORB and island arc tholeiites (Suen *et al.*, 1979; Sun *et al.*, 1979; Alabaster *et al.*, 1982). The contribution of a 'subduction component' to the incompatible element composition is less significant than in Ochi, but the (La/Nb)_{CN}

value is higher than in N-MORB and ranges from 1.2 to 1.7. The characteristics of metagabbro Et 48 are identical to those of tholeiites from oceanic island arcs at the early stages of subduction (Pearce, 1983; Pearce *et al.*, 1984).

The chemical composition data thus indicate the following scenario for the geochemical evolution of the Mt. Ochi and Tsaki ophiolitic suites: (i) the strong correlation of Cr and Ni with Mg number in Ochi rocks reflects the precipitation of olivine and possibly of Cr-spinel and clinopyroxene, to form a suite of ultrabasic to basic rocks; this genetic trend is not shown by the less-fractionated Tsaki rocks; (ii) basalts and, to a lesser extent, gabbros were hydrothermally altered by seawater; this alteration is best shown by the extremely Na- and Fe-enriched pillow rims in Ochi; (iii) REE and other incompatible element contents of Ochi basalts indicate an enriched mantle source, such as E-type MORB; Ochi basalts are thus distinguished from other southern Evia metabasites, which are characterized by either N-type MORB composition (Tsaki gabbros) or mildly enriched REE patterns; (iv) the marked negative Nb anomalies in

Table 4. (Cont.)
(b) Tsaki ophiolitic mélange.

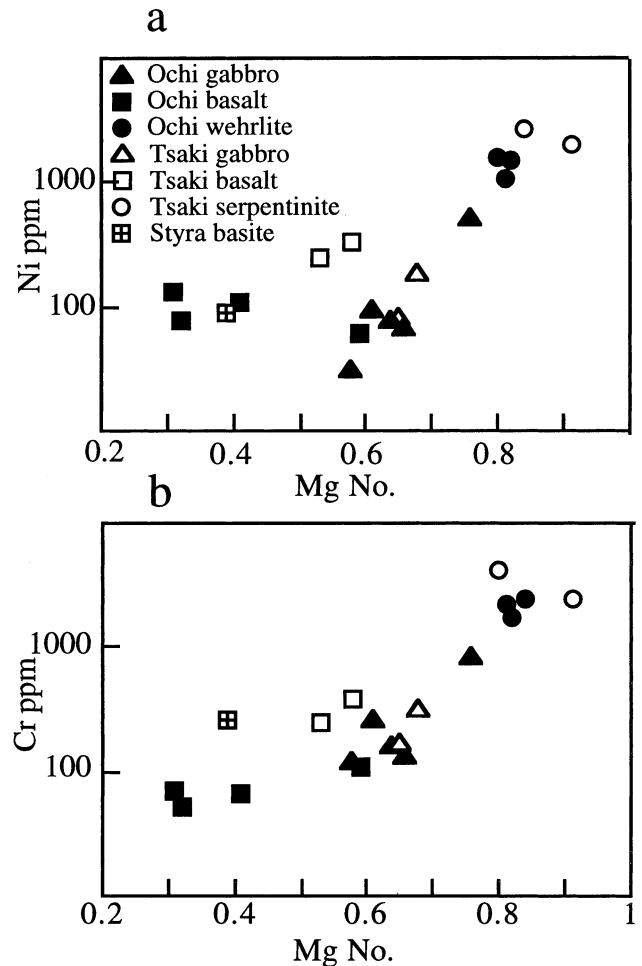
wt%	Et 47	Et 48	Et 51	Et 54	Et 115
SiO ₂	50.0	46.0	50.0	48.3	40.6
Al ₂ O ₃	15.06	14.40	12.60	15.90	1.30
Fe ₂ O ₃	9.03	9.08	15.26	10.92	7.36
TiO ₂	0.69	1.05	1.80	0.93	0.01
CaO	11.80	14.30	4.83	9.66	0.03
MgO	8.30	9.76	8.58	7.59	37.6
MnO	0.18	0.23	0.17	0.17	0.13
Na ₂ O	3.25	1.30	4.18	4.02	0.02
K ₂ O	0.13	0.67	0.21	0.44	0.02
P ₂ O ₅	0.1	0.2	<0.1	0.2	<0.1
LOI	1.81	3.15	2.64	2.52	12.42
Total	100.35	100.14	100.27	100.65	99.49
ppm					
Ba	19	72	27	58	
Cr	165	320	243	394	2645
Nb	1.4	2.6	25.0	3.7	
Ni	83	134	252	325	2000
Rb	2	15	7	12	
Sr	130	75	50	108	
Ta	0.3	0.5	2.0	0.5	
Th	0.6	0.6	2.8	0.7	
Y	19	26	13	20	
La	2	3	9	6	
Ce	5	8	22	14	
Pr	0.8	1.4	2.9	2.0	
Nd	4.4	7.8	13.0	10.0	
Sm	1.6	2.8	3.0	2.8	
Eu	0.6	1.0	0.7	1.1	
Gd			2.3	2.6	
Tb	0.4	0.6	0.4	0.5	
Dy	2.8	4.1	2.4	3.3	
Ho	0.6	0.9	0.5	0.7	
Er	1.9	2.6	1.5	2.0	
Tm	0.3	0.4	0.2	0.3	
Yb	1.9	2.5	1.6	1.7	
Lu	0.3	0.4	0.3	0.3	

Et 47, Et 48, Tsaki metagabbro; Et 51, Et 54, Tsaki metabasalts; Et 115, Tsaki serpentinite.

Ochi and Tsaki rocks indicate origin above a subduction zone.

Oxygen isotope composition

The oxygen isotope analyses of minerals of the metagabbros and a metabasalt are given in Table 3 and illustrated in Fig. 16. Relict augite from the gabbros of Mt. Ochi analyse between 5.2 and 6.4‰, and are close to the values anticipated for primary igneous ocean floor gabbros. Hornblende formed during high-temperature sea floor alteration has similar values to augite, but M1 and M2 minerals give somewhat higher $\delta^{18}\text{O}$ values between 8 and 12‰. The Tsaki minerals (altered hornblende and M2 pumpellyite) give the highest $\delta^{18}\text{O}$ values at *c.* 13‰. The significance of these differences in isotopic composition can be appreciated by comparison with the $\delta^{18}\text{O}$ values of M1 metagabbros on Syros, where relict amphibole formed during sea floor metamorphism typically has $\delta^{18}\text{O}$ values $\leq 6\text{‰}$, and high-pressure minerals, such as glaucophane, omphacite and garnet, have values of 4.2–7.1‰, 3.5–6.1‰ and 2.6–5.9‰, respectively (Putlitz *et al.*, 2000). These low $\delta^{18}\text{O}$ values reflect the high-temperature sea floor alteration frequently observed in the gabbros of intact ophiolites

**Fig. 13.** Variation diagrams of the compatible trace elements Ni (a) and Cr (b) versus Mg number in southern Evia metabasites.

and modern sea floor (e.g. Gregory & Taylor, 1981; Ito & Clayton, 1983; Stakes, 1991; Stakes *et al.*, 1991). This situation clearly does not occur in the Evia metagabbros where the M1 minerals possess significantly higher $\delta^{18}\text{O}$ values (Fig. 16). This suggests that metamorphic fluid–rock interaction during or prior to M1 metamorphism has led to ^{18}O enrichment of the M1 minerals. This is particularly evident in the $\delta^{18}\text{O}$ values of the metagabbros of Mt. Ochi where M1 glaucophane, with ^{18}O values between 9 and 11‰, texturally overgrows augite with igneous $\delta^{18}\text{O}$ values (Fig. 5c). The most likely process for this isotopic enrichment is the infiltration of high- $\delta^{18}\text{O}$ fluids derived from dehydration reactions in the metasediments enclosing the gabbros. The high LILE contents of Ochi metagabbros (Fig. 15) may also result from the infiltration of fluids bearing a geochemical signature of sedimentary rocks. The oxygen isotope results thus agree with the whole-rock geochemical data, indicating that the metagabbros experienced metasomatic change, and further indicate that this was most likely associated with M1 metamorphism.

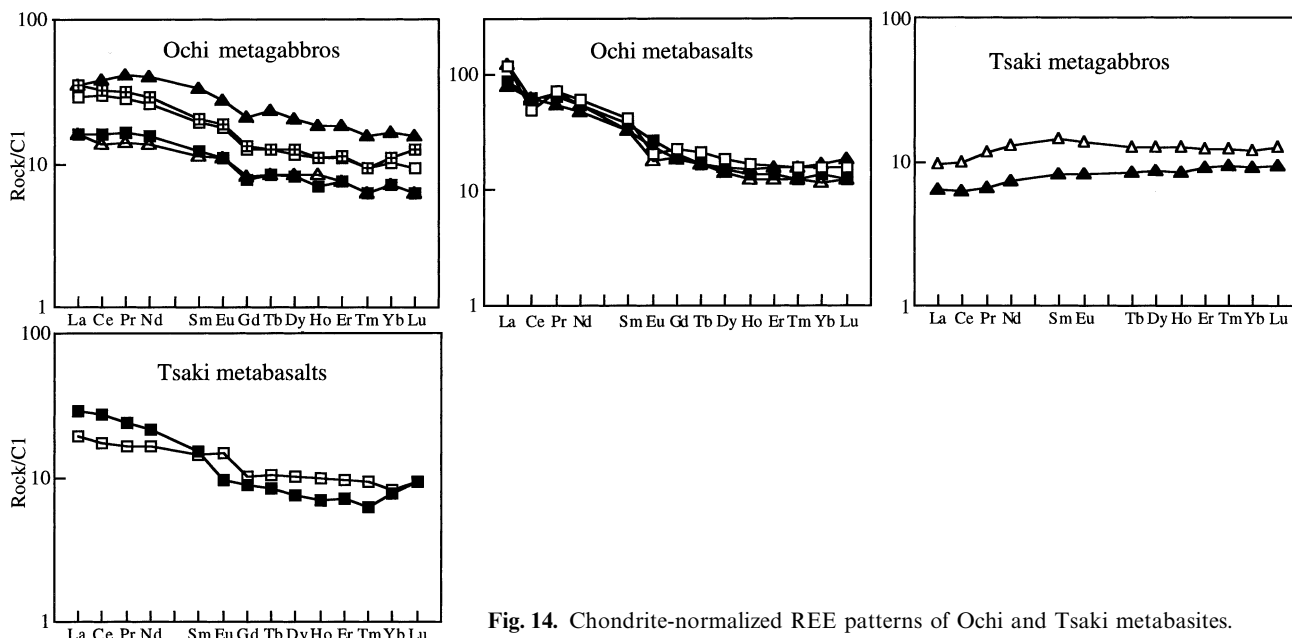


Fig. 14. Chondrite-normalized REE patterns of Ochi and Tsaki metabasites.

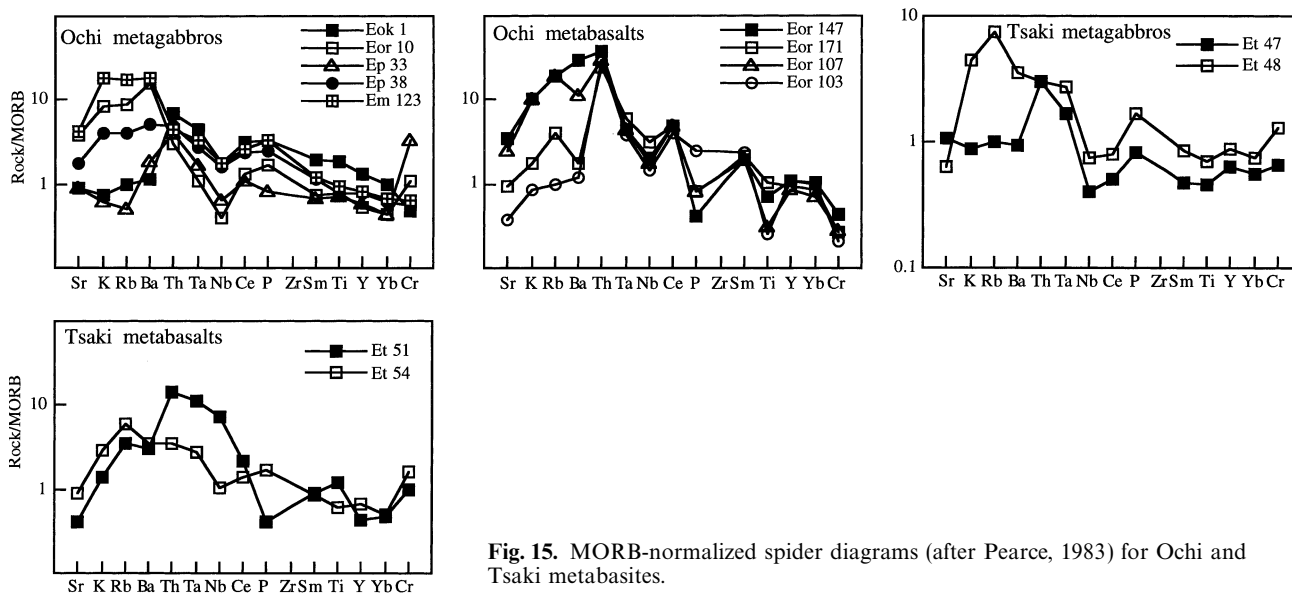


Fig. 15. MORB-normalized spider diagrams (after Pearce, 1983) for Ochi and Tsaki metabasites.

The fluid infiltration into the Mt. Ochi gabbros would have been assisted by the syn M1 deformation, which would have helped to create a deformation-enhanced permeability (e.g. Rumble, 1994; Oliver, 1996). The direct overgrowth of igneous augite by M1 minerals suggests that the gabbroic body did not experience extensive sub-sea floor hydrothermal alteration. However, in order to develop the epidote-blueschist assemblage (2.5–4 wt% H_2O), fluid infiltration was a necessary requisite. Thus the deformation-enhanced fluid infiltration from dehydrating metasediments could have served as the control of

the M1 metamorphic assemblage development in the Ochi gabbroic block.

The M2 minerals at Mt. Ochi and Paradisi have $\delta^{18}O$ values similar to those of the M1 minerals (Fig. 16). This suggests that the mineral growth of the pumpellyite- and actinolite-bearing assemblages during M2 metamorphism was influenced by fluids that were remobilized during the reactions of M1 minerals, i.e. there was no substantial infiltration of an external fluid. The Tsaki M2 assemblage of altered hornblende and pumpellyite gives unusually high $\delta^{18}O$ values (Fig. 16). The minerals are taken from sheared gabbros

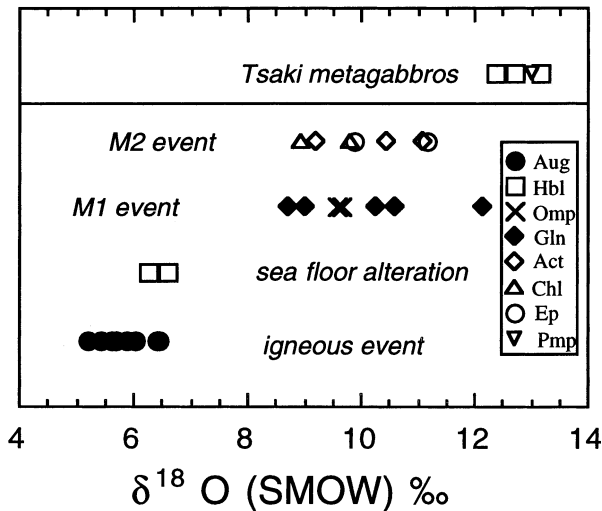


Fig. 16. Oxygen isotope analyses of minerals of metagabbros and one metabasalt from Ochi and Tsaki ophiolitic mélanges.

at the base of the Tsaki Unit and their high $\delta^{18}\text{O}$ possibly reflects extensive shear zone remobilization of fluids from the underlying metasedimentary rocks. Similar high $\delta^{18}\text{O}$ values have been reported for shear zone minerals on Tinos island (Katzir *et al.*, 1996).

DISCUSSION

Parent igneous structures, textures and mineralogy preserved within the southern Evia blueschists allow the definition of the environment in which the protoliths were formed. The igneous rocks enclosed in the Ochi mélangé are representative of the oceanic lithosphere, including pillow basalts, gabbros and wehrlites. Wehrlites are thought to originate either by precipitation from a magma (Elthon *et al.*, 1982; Smewing *et al.*, 1984) or by magmatic impregnation and dyke and sill injection into mantle peridotites (Nicolas & Prinzhofer, 1983). Wehrlitic dykes, rooted at the Moho and intruded into the crustal gabbro section, were observed at the Oman ophiolite and interpreted as a crystal melt mixture composed of basaltic melt and mantle xenocrysts (Benn *et al.*, 1988). The wehrlitic lens characterized by cumulate olivine and the large gabbroic body intruded by wehrlitic dyke at Mt. Ochi were thus probably derived from the lowermost part of the oceanic crust and the mantle–crust transition zone. The Tsaki ophiolitic mélangé, on the other hand, includes gabbros and basalts as well as large bodies of serpentinized harzburgite, representing a residual oceanic mantle from which basaltic melt has been extracted. This deep component of ophiolite suites is absent in the Ochi ophiolitic mélangé.

There is clear evidence that the igneous bodies were incorporated into the enclosing sedimentary sequence prior to peak metamorphism: (i) the foliation in the metasedimentary rocks wraps and in places penetrates

the meta-igneous bodies; (ii) metasomatic reaction zones developed through cation diffusion at peak temperatures envelope the ultrabasic bodies and follow their current geometry; (iii) M1 peak metamorphic conditions recorded in the igneous bodies and in the sedimentary country rocks are similar; (iv) fluid infiltration from the metasediments into the metagabbroic rocks occurred during M1 metamorphism.

The P – T path indicated for the ophiolitic mélanges in southern Evia is shown in Fig. 17. The data show that the metabasic and metasedimentary rocks were metamorphosed within the epidote–blueschist facies field at maximum temperatures of *c.* 450 °C and pressures ≥ 11.5 kbar. The M1 minimum pressures in southern Evia are not different from those determined throughout the NW Cyclades: omphacite of at least 60 mol.% jadeite occurs in either quartz-bearing metabasites or ferromanganous quartzites in the Central Eclogite Axis (CEA) and Andros as well as in southern

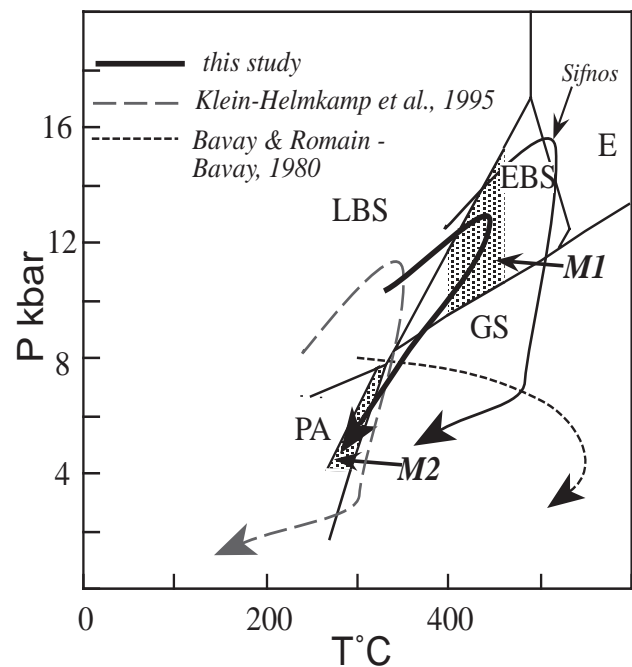


Fig. 17. P – T path of Evian blueschists based on our petrological observations and calculations for M1 and M2 assemblages (Figs 11 & 12). M1 temperatures on Evia are slightly lower than those determined in the 'Central Eclogite Axis' of the Cycladic Massif (e.g. Sifnos; Matthews & Schliestedt, 1984; Avigad *et al.*, 1992). Evian rocks were metamorphosed at epidote–blueschist facies conditions, with relict lawsonite that represents an earlier stage of their prograde path. Cooling during decompression of Evian blueschists, deduced from M2 overprinting pumpellyite–actinolite assemblages, requires further refrigeration than shown by the retrograde trajectories on Sifnos and that suggested previously for Evia (Klein-Helmkamp *et al.*, 1995), which are characterized by isothermal decompression.

Evia (Reinecke, 1986; Schliestedt, 1986; Dixon & Ridley, 1987; Bröcker *et al.*, 1993; Buzaglo-Yoresh *et al.*, 1995). Moreover, jadeite (Jd_{92}) occurs in metaacidites both in the NW Cyclades and in southern Evia (Schliestedt *et al.*, 1987; Okrusch & Bröcker, 1990; Buzaglo-Yoresh *et al.*, 1995). We thus conclude that the rocks exposed throughout the N Cyclades, from the CEA (Sifnos–Syros–Tinos) via Andros to southern Evia, represent a crustal section metamorphosed at pressures of >11 kbar during continental collision. Temperatures across this subducted crustal section vary, and a temperature difference (*c.* 50°C) between southern Evia rocks and those of the NW Cycladic islands is inferred from thermometric studies. This temperature difference is supported by other data. Lawsonite is preserved in variable rock types in Evia, whereas in the CEA its existence in pre-peak M1 assemblages is inferred by the occurrence of pseudomorphs of white mica and epidote (Okrusch & Bröcker, 1990). Igneous and ocean floor hydrothermal relics, clinopyroxene and amphibole, respectively, are well preserved in metagabbro, metabasalt and meta-vehlite of southern Evia ophiolitic mélanges, whereas in the NW Cyclades oceanic mineralogical relics are solely preserved in the N Syros metagabbro (Dixon & Ridley, 1987; Seck *et al.*, 1996; Putlitz *et al.*, 2000). The extensive preservation of igneous mineralogy is a clear indicator for the lower temperature nature of M1 in southern Evia. Spessartine-bearing Mn-rich quartzites from Andros indicate higher metamorphic temperatures than their sursassite-bearing counterparts in southern Evia (Reinecke, 1986). Finally, temperatures calculated by quartz mineral oxygen isotope thermometry are 480°C on Sifnos, 470°C on Tinos and 430°C in southern Evia (Bröcker *et al.*, 1993; Matthews, 1994; this study).

There are two possible ways to interpret the M1 P – T estimates in southern Evia. In the first interpretation, peak pressures, like temperatures, were slightly lower in southern Evia compared to the N Cyclades. Consequently, Evian blueschists were subducted to slightly shallower levels than the Cycladic eclogites, and both terranes show similar P – T trajectories. Alternatively, Evian blueschists and Cycladic eclogites represent the same depth interval of the subducted plate; however, the latter lingered longer in deep crustal levels, allowing prolonged heating. Thus, in the second interpretation, Evian blueschist stayed at depths for a shorter time and did not equilibrate to ambient temperatures.

During the Upper Cretaceous–mid-Eocene–Early Miocene time interval, the blueschists in southern Evia decompressed from *c.* 11 kbar to at least 7 kbar. Whereas in the NW Cyclades blueschists and eclogites were decompressed isothermally through greenschist facies conditions (Matthews & Schliestedt, 1984; Avigad *et al.*, 1992; Bröcker *et al.*, 1993), decompression in southern Evia involved cooling from epidote–blueschist conditions ($T_{\text{max}}=450^\circ\text{C}$) to pumpellyite–

actinolite facies conditions ($T_{\text{max}}=350^\circ\text{C}$). The decompressional cooling of southern Evian rocks cannot be explained, however, either by return laminar flow in mélange channels (Franciscan complex; Cloos, 1984) or by syn-orogenic extensional detachments, thought to induce cooling in the upper parts of the exhumed footwall (Crete, Oman; Jolivet *et al.*, 1998). The Franciscan-type exhumation model is ruled out by the origin, field relations and distribution of the Evian mélanges shown in this work. Correspondingly, the detachments that delimit the Cycladic Blueschist Unit from above are shown to reflect post-orogenic back arc extension (Avigad *et al.*, 1997; Patriat & Jolivet, 1998), which does not produce the anticipated differential cooling (Ruppel *et al.*, 1988; Hodges *et al.*, 1996; Morrison & Lawford Anderson, 1998). A possible mechanism to account for the decompressional cooling (and for the lower M1 temperatures), which distinguishes southern Evian blueschists from most of the other Cycladic high- P/T rocks, is continuous accretion of relatively cold rocks at the bottom of the Blueschist Unit (e.g. Rubie, 1984; see also Matthews *et al.*, 1999). Our petrological analysis indicates that the M2 pumpellyite–diopside paragenesis of Tsaki metabasites at the base of the section equilibrated at temperatures slightly lower than those indicated by the pumpellyite–actinolite assemblage of overlying Ochi metabasites, which occur *c.* 2 km above, near the top of the section. This decrease in M2 temperatures downwards towards the base of the Blueschist Unit can be explained by the underthrusting of the Late Eocene sedimentary rocks of the Almyropotamos platform beneath the Blueschist Unit, which has either caused cooling by conduction, or resulted in a more prolonged retrograde metamorphism impelled by the infiltration of fluids from below. The 12–13‰ oxygen isotopic compositions of M2 minerals from Tsaki metagabbros are slightly higher than those of the Ochi minerals, suggesting the presence of a high- $\delta^{18}\text{O}$ fluid phase during their crystallization. These fluids could have been derived from devolatilization of metapelitic rocks of the Tsaki Unit or the Almyropotamos flysch, which occurred during continued underthrusting. Deformation-enhanced fluid infiltration through a basal thrust is also thought to account for a gradient in Rb–Sr ages from top (*c.* 40 Ma) to bottom (*c.* 22 Ma) in the Cycladic Blueschist Unit of Tinos (Bröcker & Franz, 1998). This shows that underthrusting and fluid infiltration from below are processes of major regional importance throughout the exhumation of the Cycladic blueschists.

In conclusion, exhumation of the Blueschist Unit in southern Evia from depths of 40 km to the surface involved crustal accretion below it, cooling during decompression and an inverted temperature gradient within it. These three features are characteristic of an active accretionary wedge environment, and indicate that a substantial part of the exhumation of the Evian blueschists occurred during convergent tectonics.

ACKNOWLEDGEMENTS

The petrological and field studies were supported by a grant to D. Avigad from the United States–Israel Binational Science Foundation (BSF), Jerusalem. The geochemical and isotopic studies and the laser fluorination system were supported by grants to A. Matthews from the United States–Israel Binational Science Foundation (BSF) and the Israel Science Foundation funded by the Israel Academy of Sciences and Humanities. Dr. B. Putlitz is kindly thanked for performing the laser probe analysis, A. Mor for producing high-quality mineral separates from difficult rocks, E. Yizraeli for helping with the Raman spectrometer, and V. Gutkin for help with the electron microprobe. We would like to thank the Geochemistry Division of the Geological Survey of Israel for the chemical analyses and S. Ehrlich and Dr. O. Yoffe for performing the analytical work. Thanks are also due to N. Lensky and Y. Shaked for kind help and creative ideas in the field. Discussions with E. Humler, K. Gillis, G. Godard, C. Mével and O. Navon are appreciated. We thank J. Dixon for an exhaustive review of an earlier version of the manuscript. Critical reviews by M. Bröcker, S. Maruyama, M. Schliestedt and J. Schumacher significantly contributed to the improvement of this paper. Permission for fieldwork in Greece was granted by the director of the Institute of Geological and Mining Research (I.G.M.E.) in Athens.

REFERENCES

- Alabaster, T., Pearce, J. A. & Malpas, J., 1982. The volcanic stratigraphy and petrogenesis of the Oman ophiolite complex. *Contributions to Mineralogy and Petrology*, **81**, 168–183.
- Altherr, R., Schliestedt, M., Okrusch, M., Seidel, E., Kreuzer, H., Harre, W., Lenz, H., Wendt, I. & Wagner, G. A., 1979. Geochronology of high pressure rocks on Sifnos (Cyclades, Greece). *Contributions to Mineralogy and Petrology*, **70**, 245–255.
- Avigad, D. & Garfunkel, Z., 1989. Low-angle faults above and below a blueschist belt—Tinos Island, Cyclades, Greece. *Terra Nova*, **1**, 182–187.
- Avigad, D. & Garfunkel, Z., 1991. Uplift and exhumation of high-pressure metamorphic terrains: the example of the Cycladic blueschist belt (Aegean Sea). *Tectonophysics*, **188**, 357–372.
- Avigad, D., Garfunkel, Z., Jolivet, L. & Azañon, J. M., 1997. Back arc extension and denudation of Mediterranean eclogites. *Tectonics*, **16**, 924–941.
- Avigad, D., Matthews, A., Evans, B. W. & Garfunkel, Z., 1992. Cooling during the exhumation of a blueschist terrane: Sifnos (Cyclades), Greece. *European Journal of Mineralogy*, **4**, 619–634.
- Banno, S., 1998. Pumpellyite–actinolite facies of the Sanbagawa metamorphism. *Journal of Metamorphic Geology*, **16**, 117–128.
- Bavay, P. & Romain-Bavay, D., 1980. L'unité de Styra-Ochi: un ensemble métamorphique de type schistes bleus d'âge alpin dans le massif d'Attique-Cyclades (Eubée du Sud, Grèce). *These 3ème cycle, Université de Paris-Sud, Paris*.
- Benn, K., Nicolas, A. & Reuber, I., 1988. Mantle-crust transition zone and origin of wehrlicite magmas: evidence from the Oman ophiolite. *Tectonophysics*, **151**, 75–85.
- Blake, M. C., Bonneau, M., Geysant, J., Kienast, J. R., Lepvrier, C., Maluski, H. & Papanikolaou, D., 1981. A geologic reconnaissance of the Cycladic blueschist belt, Greece. *Geological Society of America Bulletin*, **192**, 247–254.
- Bonneau, M. & Kienast, J. R., 1982. Subduction, collision et schistes bleus: l'exemple de l'Egee (Grèce). *Bulletin de la Société Géologique de France*, **7**, 785–792.
- Boynton, W. V., 1984. Geochemistry of the rare earth elements: meteorite studies. In: *Rare Earth Element Geochemistry* (ed. Henderson, P.), pp. 63–114. Elsevier, Amsterdam.
- Bröcker, M., 1991. Geochemistry of metabasic HP/LT rocks and their greenschist facies and contact metamorphic equivalents, Tinos Island (Cyclades, Greece). *Chemie der Erde*, **51**, 155–171.
- Bröcker, M. & Enders, M., 1999. U–Pb zircon geochronology of unusual eclogite-facies rocks from Syros and Tinos (Cyclades, Greece). *Geological Magazine*, **136**, 111–118.
- Bröcker, M. & Franz, L., 1998. Rb–Sr isotope studies on Tinos Island (Cyclades, Greece): additional time constraints for metamorphism, extent of infiltration-controlled overprinting and deformational activity. *Geological Magazine*, **135**, 369–382.
- Bröcker, M., Kreuzer, A., Matthews, A. & Okrusch, M., 1993. ⁴⁰Ar/³⁹Ar and oxygen isotope studies of poly-metamorphism from Tinos Island, Cycladic blueschist belt, Greece. *Journal of Metamorphic Geology*, **11**, 223–240.
- Buick, I. S., 1991. The late Alpine evolution of an extensional shear zone, Naxos, Greece. *Journal of the Geological Society, London*, **148**, 93–103.
- Buzaglo-Yoresh, A., Matthews, A. & Garfunkel, Z., 1995. Metamorphic evolution on Andros and Tinos – a comparative study. In: *Israel Geological Society Annual Meeting 1995* (eds Arkin, Y. & Avigad, D.), pp. 16. Israel Geological Society, Jerusalem.
- Cloos, M., 1984. Flow melanges and the structural evolution of accretionary wedges. In: *Melanges: Their Nature, Origin and Significance* (ed. Raymond, L. A.), pp. 71–79. Geological Society of America, Boulder, CO, USA, Special Paper 198.
- Coombs, D. S., Nakamura, Y. & Vuagnat, M., 1976. Pumpellyite–actinolite facies schists of the Taveyenne formation near Loèche, Valais, Switzerland. *Journal of Petrology*, **17**, 440–471.
- Dixon, J. E. & Ridley, J., 1987. Syros. In: *Chemical Transport in Metasomatic Processes* (ed. Helgeson, H. C.), pp. 489–501. NATO ASI Series, Reidel, Dordrecht.
- Dubois, R. & Bignot, G., 1979. Présence d'un 'hardground' nummulitique au de la série Crétacée d'Almyropotamos (Eubée méridionale, Grèce). *Comptes Rendus de l'Académie des Sciences (Paris), Ser. II*, **289**, 993–995.
- Dürr, S., Altherr, R., Keller, J., Okrusch, M. & Seidel, E., 1978. The median Aegean crystalline belt: stratigraphy, structure, metamorphism, magmatism. In: *Alps, Appenines, Hellenides* (eds Closs, H., Roeder, D. H. & Schmidt, K.), pp. 455–477. Inter-Union Commission on Geodynamics (I.U.G.S.) Report 38, Schweizerbart, Stuttgart.
- Elthon, D., Casey, J. F. & Komor, S., 1982. Mineral chemistry of ultramafic cumulates from the North Arm Mountain Massif of the Bay of Island ophiolite, Newfoundland: evidence for high pressure crystal fractionation of oceanic basalts. *Journal of Geophysical Research*, **87**, 8717–8734.
- Evans, B. W., 1977. Metamorphism of Alpine peridotite and serpentinite. *Annual Reviews in Earth and Planetary Science*, **5**, 397–447.
- Evans, B. W., 1990. Phase relations of epidote–blueschists. *Lithos*, **25**, 3–23.
- Frost, B. R., 1975. Contact metamorphism of serpentinite, chloritic blackwall and rodingite at Paddy-Go-Easy pass, Central Cascades, Washington. *Journal of Petrology*, **16**, 272–312.
- Gautier, P. & Brun, J. P., 1994. Crustal-scale geometry and kinematics of late-orogenic extension in the central Aegean (Cyclades and Evvia Island). *Tectonophysics*, **238**, 399–424.
- Gregory, R. T. & Taylor, H. P., 1981. An oxygen isotope profile in a section of Cretaceous oceanic crust, Samail ophiolite, Oman: evidence for ¹⁸O buffering of the oceans by deep (>5 km) seawater-hydrothermal circulation at mid-ocean ridges. *Journal of Geophysical Research*, **86B**, 2737–2755.

- Hawkesworth, C. J., Gallagher, K., Hergt, J. M. & McDermott, F., 1993. Mantle and slab contributions in arc magmas. *Annual Reviews in Earth and Planetary Science*, **21**, 175–204.
- Hodges, K., Parrish, R. R. & Searle, M. P., 1996. Tectonic evolution of the Central Annapurna Range. *Tectonics*, **15**, 1264–1291.
- Holland, T. J. B. & Powell, R., 1998. An internally consistent thermodynamic data set for phases of petrological interest. *Journal of Metamorphic Geology*, **16**, 309–343.
- Ito, E. & Anderson, A. T. Jr., 1983. Submarine metamorphism of gabbros from the Mid-Cayman Rise: petrographic and mineralogic constraints on hydrothermal processes at slow-spreading ridges. *Contributions to Mineralogy and Petrology*, **82**, 371–388.
- Ito, E. & Clayton, R. N., 1983. Submarine metamorphism of gabbros from the Mid-Cayman Rise: an oxygen isotope study. *Geochimica et Cosmochimica Acta*, **47**, 535–546.
- Jacobshagen, V., 1986. *Geologie Von Griechenland*. Gebrüder Borntraeger, Berlin.
- Jolivet, L., Goffé, B., Bousquet, R., Oberhänsli, R. & Michard, A., 1998. Detachments in high-pressure mountain belts, Tethyan examples. *Earth and Planetary Science Letters*, **160**, 31–47.
- Jolivet, L. & Patriat, M., 1999. Ductile extension and the formation of the Aegean Sea. In: *The Mediterranean Basins: Tertiary Extension Within the Alpine Orogen* (eds Durand, B., Jolivet, L., Horváth, F. & Séranne, M.), pp. 427–456. Geological Society Special Publications, 156, London.
- Katsikatos, G., Migros, G., Triantaphyllis, M. & Mettos, A., 1986. Geological structure of the internal Hellenides (E. Thessaly-SW Macedonia, EoBoea-Attica-Northern Cyclades islands and Lesvos). In: *Geological and Geophysical Research*, pp. 191–212. Institute of Geological and Mining Research (I.G.M.E.), Athens.
- Katsikatos, G., 1991. *Geological Map of Greece, Rafina Sheet*. Institute of Geological and Mining Research (I.G.M.E.), Athens.
- Katzir, Y., Matthews, A., Garfunkel, G., Schliestedt, M. & Avigad, D., 1996. The tectono-metamorphic evolution of a dismembered ophiolite (Tinos, Cyclades, Greece). *Geological Magazine*, **133**, 237–254.
- Klein-Helmkamp, U., Reinecke, T. & Stöckhert, B., 1995. The aragonite–calcite transition in *LT-HP* metamorphic carbonatic rocks from S-Evia, Greece: the microstructural and compositional record. *Bochumer Geologische und Geotechnische Arbeiten*, **44**, 78–83.
- Leake, B. E., Woolley, A. R. *et al.*, 1997. Nomenclature of amphiboles: Report of the subcommittee on amphiboles of the International Mineralogical Association, commission on new minerals and mineral names. *Canadian Mineralogist*, **35**, 219–246.
- Lensky, N., Avigad, D., Garfunkel, Z. & Evans, B. W., 1997. The tectono-metamorphic evolution of blueschists in south Evia, Hellenide orogenic belt (Greece). In: *Israel Geological Society Annual Meeting 1997* (eds Sivan, D. *et al.*), pp. 66–67. Israel Geological Society, Jerusalem.
- Lister, G. S., Banga, G. & Feenstra, A., 1984. Metamorphic core complexes of Cordilleran type in the Cyclades, Aegean Sea, Greece. *Geology*, **12**, 221–225.
- Liou, J. G. & Maruyama, S., 1987. Parageneses and compositions of amphiboles from Franciscan jadeite–glaucofanite type facies series metabasites at Cazadero, California. *Journal of Metamorphic Geology*, **5**, 371–395.
- Liou, J. G., Maruyama, S. & Cho, M., 1987. Very low-grade metamorphism of volcanic and volcanoclastic rocks – mineral assemblages and mineral facies. In: *Low Temperature Metamorphism* (ed. Frey, M.), pp. 59–113. Blackie, Glasgow.
- Maluski, H., Bonneau, M. & Kienast, J. R., 1987. Dating metamorphic events in the Cycladic area: $^{39}\text{Ar}/^{40}\text{Ar}$ data from metamorphic rocks of the island of Syros (Greece). *Bulletin de la Société Géologique de France*, **8**, 833–842.
- Maluski, H., Vergely, P., Bavay, D., Bavay, P. & Katsikatos, G., 1981. $^{39}\text{Ar}/^{40}\text{Ar}$ dating of glaucophanes and phengites in Southern Euboa (Greece), geodynamic implications. *Bulletin de la Société Géologique de France*, **7**, 469–476.
- Maruyama, S. & Liou, J. G., 1985. The stability of Ca–Na pyroxene in low-grade metabasites of high-pressure intermediate facies series. *American Mineralogist*, **70**, 16–29.
- Maruyama, S. & Liou, J. G., 1987. Clinopyroxene—a mineral telescoped through the processes of blueschist facies metamorphism. *Journal of Metamorphic Geology*, **5**, 529–552.
- Massonne, H. J. & Schreyer, W., 1987. Phengite geobarometry based on the limiting assemblage with K-feldspar, phlogopite, and quartz. *Contributions to Mineralogy and Petrology*, **96**, 212–224.
- Matthews, A., 1994. Oxygen isotope geothermometers for metamorphic rocks. *Journal of Metamorphic Geology*, **12**, 211–219.
- Matthews, A., Lieberman, J. L., Avigad, D. & Garfunkel, Z., 1999. Fluid rock interaction and thermal evolution during thrusting in an Alpine metamorphic complex (Tinos Island, Greece). *Contributions to Mineralogy and Petrology*, **135**, 212–224.
- Matthews, A. & Schliestedt, M., 1984. Evolution of the blueschist and greenschist facies rocks of Sifnos, Cyclades, Greece. *Contributions to Mineralogy and Petrology*, **88**, 150–163.
- Michard, A., 1989. Rare earth element systematics in hydrothermal fluids. *Geochimica et Cosmochimica Acta*, **53**, 745–750.
- Monnier, C., Girardeau, J., Maury, R. C. & Cotten, J., 1995. Back-arc basin origin for the East Sulawesi ophiolite (eastern Indonesia). *Geology*, **23**, 851–854.
- Morimoto, N., 1988. Nomenclature of pyroxenes. *Mineralogical Magazine*, **52**, 535–550.
- Morrison, J. & Lawford Anderson, J., 1998. Footwall refrigeration along a detachment fault: implications for the thermal evolution of core complexes. *Science*, **279**, 63–66.
- Nakajima, T., Banno, S. & Suzuki, T., 1977. Reactions leading to the disappearance of pumpellyite in low-grade metamorphic rocks of the Sanbagawa metamorphic belt in central Shikoku, Japan. *Journal of Petrology*, **18**, 263–284.
- Nicolas, A. & Prinzhofer, A., 1983. Cumulative or residual origin for the transition zone in ophiolites: structural evidence. *Journal of Petrology*, **24**, 188–206.
- O'Hanley, D. S., 1996. *Serpentinites, Records of Tectonic and Petrological History*. Oxford University Press, New York.
- Okrusch, M. & Bröcker, M., 1990. Eclogites associated with high-grade blueschists in the Cyclades archipelago, Greece: a review. *European Journal of Mineralogy*, **2**, 451–478.
- Oliver, N. H. S., 1996. Review and classification of structural controls on fluid flow during regional metamorphism. *Journal of Metamorphic Geology*, **14**, 477–492.
- Papanikolaou, D., 1987. Tectonic evolution of the Cycladic blueschist belt (Aegean Sea, Greece). In: *Chemical Transport in Metasomatic Processes* (ed. Helgeson, H. C.), pp. 429–450. NATO ASI Series, Reidel, Dordrecht.
- Patriat, M. & Jolivet, L., 1998. Post-orogenic extension and shallow-dipping shear zones, study of a brecciated decollement horizon in Tinos (Cyclades, Greece). *Comptes Rendus de l'Académie des Sciences, Paris*, **326**, 355–362.
- Patrick, B. E. & Evans, B. W., 1989. Metamorphic evolution of the Seward Peninsula blueschist terrane. *Journal of Petrology*, **30**, 531–555.
- Pearce, J. A., 1983. Role of sub-continental lithosphere in magma genesis at active continental margins. In: *Continental Basalts and Mantle Xenoliths* (eds Hawkesworth, C. J. & Norry, M. J.), pp. 230–249. Shiva Publishing, Nantwich.
- Pearce, J. A., Lippard, S. J. & Roberts, S., 1984. Characteristics and tectonic significance of supra-subduction zone ophiolites. In: *Marginal Basin Geology* (eds Kokelaar, B. P. & Howells, M. F.), pp. 77–94. Geological Society Special Publications 16, London.
- Pinsent, R. H. & Hirst, D. M., 1977. The metamorphism of Blue River ultramafic body, Cassiar, British Columbia, Canada. *Journal of Petrology*, **18**, 567–594.
- Putlitz, B., Matthews, A. & Valley, J. W., 2000. Oxygen and hydrogen isotope study of high-pressure metagabbros and

- metabasalts (Cyclades, Greece): implications for the subduction of oceanic crust. *Contributions to Mineralogy and Petrology*, **138**, 114–126.
- Reinecke, T., 1982. Cymrite and celsian in manganese-rich metamorphic rocks from Andros island, Greece. *Contributions to Mineralogy and Petrology*, **79**, 333–336.
- Reinecke, T., 1986. Phase relationships of sursassite and other Mn-silicates in highly oxidized low-grade, high-pressure metamorphic rocks from Evvia and Andros Islands, Greece. *Contributions to Mineralogy and Petrology*, **94**, 110–126.
- Ridley, J., 1984. Listric normal faulting and reconstruction of the synmetamorphic structural pile of the Cyclades. In: *The Geological Evolution of the Eastern Mediterranean* (eds Dixon, J. E. & Robertson, A. H. F.), pp. 755–762. Geological Society Special Publications 17, London.
- Rosenbaum, J. M. & Matthey, D., 1995. Equilibrium garnet–calcite oxygen isotope fractionation. *Geochimica et Cosmochimica Acta*, **59**, 2839–2842.
- Rubie, D. C., 1984. A thermal-tectonic model for high-pressure metamorphism and deformation in the Sesia Zone, Western Alps. *Journal of Geology*, **92**, 21–36.
- Rumble, D., 1994. Water circulation in metamorphism. *Journal of Geophysical Research*, **B99**, 15 499–15 502.
- Ruppel, C., Royden, L. & Hodges, K., 1988. Thermal modeling of extensional tectonics: application to pressure–temperature–time histories of metamorphic rocks. *Tectonics*, **7**, 947–957.
- Saunders, A. D. & Tarney, J., 1984. Geochemical characteristics of basaltic volcanism within back-arc basins. In: *Marginal Basin Geology* (eds Kokelaar, B. P. & Howells, M. F.), pp. 59–76. Geological Society Special Publication 16, London.
- Schliestedt, M., 1986. Eclogite–blueschist relationships as evidenced by mineral equilibria in the high-pressure metabasic rocks of Sifnos (Cycladic Islands), Greece. *Journal of Petrology*, **27**, 1437–1459.
- Schliestedt, M., Altherr, R. & Matthews, A., 1987. Evolution of the Cycladic crystalline complex: petrology, isotope geochemistry and geochronology. In: *Chemical Transport in Metasomatic Processes* (ed. Helgeson, H. C.), pp. 389–428. NATO ASI Series, Reidel, Dordrecht.
- Seck, H. A., Kötz, J., Okrusch, M., Seidel, E. & Stosch, H. G., 1996. Geochemistry of a meta-ophiolite suite: an association of metagabbros, eclogites and glaucophanites on the Island of Syros, Greece. *European Journal of Mineralogy*, **8**, 607–623.
- Shaked, Y., Avigad, D. & Garfunkel, Z., 2000. Alpine high-pressure metamorphism at the Almyropotamos window (southern Evia, Greece). *Geological Magazine*, **137**, 367–380.
- Smewing, J. D., Christensen, N. I., Bartholomew, I. D. & Browning, P., 1984. The structure of the oceanic upper mantle and lower crust as deduced from the northern section of the Oman ophiolite. In: *Ophiolites and Oceanic Lithosphere* (eds Gass, I. G., Lippard, S. J. & Shelton, A. W.), pp. 41–54. Blackwell, London.
- Stakes, D. S., 1991. Oxygen and hydrogen isotope compositions of oceanic plutonic rocks: high temperature deformation and metamorphism of oceanic layer 3. In: *Stable Isotope Geochemistry: a Tribute to Samuel Epstein* (eds Taylor, H. P., O’Neil, J. R. & Kaplan, I. R.), pp. 77–90. The Geochemical Society Special Publication No. 3, University Park, PA, USA.
- Stakes, D. S., Cannat, M., Mével, C. & Chaput, T., 1991. Metamorphic history of ODP site 735B, Southwest Indian Ocean. In: *Leg 118, Scientific Results, Proc. Ocean Drilling Program* (eds Von Herzen, R., Robinson, P. T. et al.), pp. 153–180. College Station, TX, USA, Ocean Drilling Program.
- Stakes, D. S., Shervais, J. W. & Hopson, C. A., 1984. The volcanic–tectonic cycle of the FAMOUS and AMAR Valley, Mid Atlantic Ridge (36–47°N): evidence from basalt glass and phenocryst compositional variations for a steady state magma chamber beneath the valley mid-sections, AMARS. *Journal of Geophysical Research*, **B89**, 6695–7028.
- Suen, C. J., Frey, F. A. & Malpas, J., 1979. Bay of Islands ophiolite suite, Newfoundland: petrologic and geochemical characteristics with emphasis on rare earth element geochemistry. *Earth and Planetary Science Letters*, **45**, 337–348.
- Sun, S. S. & McDonough, W. F., 1989. Chemical and isotopic systematics of oceanic basalts: implications for mantle composition and process. In: *Magmatism in the Ocean Basins* (eds Saunders, A. D. & Norry, J. M.), pp. 313–345. Geological Society Special Publication 42, London.
- Sun, S. S., Nesbitt, R. W. & Sharaskin, A. Y., 1979. Geochemical characteristics of mid-ocean ridge basalts. *Earth and Planetary Science Letters*, **44**, 119–138.
- Thompson, G., 1983. Basalt–seawater interaction. In: *Hydrothermal Processes at Seafloor Spreading Centers* (eds Rona, P. A. et al.), pp. 225–278. Plenum, New York.
- Wicks, F. J. & Whittaker, E. J. W., 1977. Serpentine textures and serpentinization. *Canadian Mineralogist*, **15**, 459–488.

Received 3 November 1999; revision accepted 30 May 2000